

 Open access • Posted Content • DOI:10.1101/757393

Octanol-water partition coefficient measurements for the SAMPL6 Blind Prediction Challenge — [Source link](#)

Mehtap Işık, Mehtap Işık, Dorothy Levorse, David L. Mobley ...+2 more authors





Institutions: Cornell University, Memorial Sloan Kettering Cancer Center, Merck & Co., University of California, Berkeley

Published on: 08 Sep 2019 - bioRxiv (Cold Spring Harbor Laboratory)

Topics: Partition coefficient

Related papers:

- [Octanol–water partition coefficient measurements for the SAMPL6 blind prediction challenge](#)
- [Prediction of n-octanol/water partition coefficients and acidity constants \(pKa\) in the SAMPL7 blind challenge with the IEFPCM-MST model](#)
- [Prediction of octanol/water partition coefficient of selected ferrocene derivatives using rekker method](#)
- [Prediction of 1 Octanol/Water Partition Coefficient of Adamantanederivatives using QSAR method](#)
- [Empirical relationships of aqueous solubility and octanol-water partition coefficient of hydrocarbons with different molecular descriptors](#)

Share this paper:    

View more about this paper here: <https://typeset.io/papers/octanol-water-partition-coefficient-measurements-for-the-4suul9bies>

Octanol-water partition coefficient measurements for the SAMPL6 Blind Prediction Challenge

Mehtap Işık (ORCID: [0000-0002-6789-952X](https://orcid.org/0000-0002-6789-952X))^{1,2}, Dorothy Levorse³, David L. Mobley (ORCID: [0000-0002-1083-5533](https://orcid.org/0000-0002-1083-5533))⁴, Timothy Rhodes (ORCID: [0000-0001-7534-9221](https://orcid.org/0000-0001-7534-9221))^{3*}, John D. Chodera (ORCID: [0000-0003-0542-119X](https://orcid.org/0000-0003-0542-119X))^{1*}

¹Computational and Systems Biology Program, Sloan Kettering Institute, Memorial Sloan Kettering Cancer Center, New York, NY 10065, United States; ²Tri-Institutional PhD Program in Chemical Biology, Weill Cornell Graduate School of Medical Sciences, Cornell University, New York, NY 10065, United States; ³Pharmaceutical Sciences, MRL, Merck & Co., Inc., 126 East Lincoln Avenue, Rahway, New Jersey 07065, United States; ⁴Department of Pharmaceutical Sciences and Department of Chemistry, University of California, Irvine, Irvine, California 92697, United States

*For correspondence:

timothy_rhodes@merck.com (TR); john.chodera@choderalab.org (JDC)

Abstract Partition coefficients describe the equilibrium partitioning of a single, defined charge state of a solute between two liquid phases in contact, typically a neutral solute. Octanol-water partition coefficients (K_{ow}), or their logarithms ($\log P$), are frequently used as a measure of lipophilicity in drug discovery. The partition coefficient is a physicochemical property that captures the thermodynamics of relative solvation between aqueous and nonpolar phases, and therefore provides an excellent test for physics-based computational models that predict properties of pharmaceutical relevance such as protein-ligand binding affinities or hydration/solvation free energies. The SAMPL6 Part II Octanol-Water Partition Coefficient Prediction Challenge used a subset of kinase inhibitor fragment-like compounds from the SAMPL6 pK_a Prediction Challenge in a blind experimental benchmark. Following experimental data collection, the partition coefficient dataset was kept blinded until all predictions were collected from participating computational chemistry groups. A total of 91 submissions were received from 27 participating research groups. This paper presents the octanol-water $\log P$ dataset for this SAMPL6 Part II Partition Coefficient Challenge, which consisted of 11 compounds (six 4-aminoquinazolines, two benzimidazole, one pyrazolo[3,4-d]pyrimidine, one pyridine, one 2-oxoquinoline substructure containing compounds) with $\log P$ values in the range of 1.95–4.09. We describe the potentiometric $\log P$ measurement protocol used to collect this dataset using a Sirius T3, discuss the limitations of this experimental approach, and share suggestions for future $\log P$ data collection efforts for the evaluation of computational methods.

0.1 Keywords

octanol-water partition coefficient · $\log P$ · blind prediction challenge · SAMPL · kinase inhibitor fragments · 4-aminoquinazoline · potentiometric $\log P$ measurement

0.2 Abbreviations

SAMPL Statistical Assessment of the Modeling of Proteins and Ligands

$\log P$ \log_{10} of the organic solvent-water partition coefficient (K_{ow} , refers to partition of neutral species unless stated otherwise)

$\log D$ \log_{10} of organic solvent-water distribution coefficient (D_{ow})

$\log R$ \log_{10} of the volumetric ratios of partition solvents (octanol to water)

pK_a $-\log_{10}$ of the acid dissociation equilibrium constant

- 39 p_oK_a $-\log_{10}$ apparent acid dissociation equilibrium constant in octanol-water biphasic system
40 **ISA** Ionic-strength adjusted solution with 0.15 M KCl
41 **SEM** Standard error of the mean
42 **LC-MS** Liquid chromatography-mass spectrometry
43 **NMR** Nuclear magnetic resonance spectroscopy
44 **HRMS** High-resolution mass spectrometry
45 **octanol** 1-octanol, also known as n-octanol

46 1 Introduction

47 The SAMPL (Statistical Assessment of the Modeling of Proteins and Ligands) Challenges [<http://sAMPLchallenges.github.io>] are a
48 series of blind prediction challenges for the computational chemistry community that aim to evaluate and advance computational
49 tools for rational drug design [1]. These challenges focus the community on specific phenomena relevant to drug discovery—such
50 as the contribution of force field inaccuracy to binding affinity prediction failures—and, using carefully-selected test systems,
51 isolate these phenomena from other confounding factors. Through recurring community exercises involving blind prediction
52 followed by data sharing and discussion, these challenges evaluate tools and methodologies prospectively, enforce data sharing
53 to learn from failures, and generate high-quality datasets into the community as benchmark sets. As a result, SAMPL has driven
54 progress in a number of areas over six previous rounds of challenge cycles [2–15].

55 To assess the accuracy of different computational methods, SAMPL has relied on the measurement of simple host-guest
56 association affinities [6, 8, 11, 15–19] and other physical properties that isolate issues such as failing to capture relevant
57 chemical effects, computationally-intensive conformational sampling, and force field accuracy. In SAMPL5, for example, a log D
58 challenge was devised with the goal of isolating the accuracy of protein-ligand force fields from the difficulties of configurational
59 sampling [20, 21]. In addition to being a useful surrogate for the accuracy of force fields in predicting binding free energies,
60 partition or distribution coefficients are frequently used as a measure of lipophilicity in pharmacology [22], or as surrogates for
61 solubility, permeability [23], and contributors to affinity [22, 24]. Lipophilicity is a critical physicochemical property that affects
62 ADMET (absorption, distribution, metabolism, excretion, and toxicity) [22, 25, 26]. Since log P is utilized as a predictor for good
63 drug-like properties in terms of pharmacokinetics and toxicity [25], accurate log P predictions of virtual molecules have high
64 potential to benefit drug discovery and design.

65 Surprisingly, the cyclohexane-water log D challenge proved to be particularly problematic due to the necessity to account for
66 protonation state effects to correctly compute the distribution coefficients, which assess the partitioning of all ionization states
67 between phases [20]; failing to account for these protonation state effects led to modeling errors up to several log units [27].
68 As a result, the SAMPL6 Part II log P Prediction Challenge [28] aimed to further isolate the assessment of force field accuracy
69 from the issues of conformational sampling and the modeling of ionization state equilibria by inviting participants to predict the
70 partitioning of *neutral* drug-like molecules between aqueous and nonaqueous phases¹. For maximum synergy with previous
71 competitions, the challenge compound set was constructed to be a subset of kinase inhibitor fragment-like small molecules drawn
72 from the SAMPL6 pK_a Challenge set [29], where the accuracy of participants to predict pK_a values was assessed. A blind challenge
73 (the SAMPL6 Part II log P Blind Prediction Challenge) was run from November 1, 2018 to March 22, 2019 in which participants were
74 given molecular structures and experimental details and asked to predict octanol-water partition coefficients before the data was
75 unblinded on March 25, 2019. All primary and processed data was made available at <https://github.com/MobleyLab/SAMPL6>
76 immediately following the close of the competition.

77 Partition coefficients and principles of their measurement

78 The partition coefficient describes the equilibrium partitioning of a molecule in a single, defined, charge state between two liquid
79 phases in contact. Unless stated otherwise, in common usage partition coefficient (P or P^0) refers to the partitioning of the neutral
80 state of a molecule. In particular, the octanol-water partition coefficient of neutral species (frequently written as K_{ow} or P) is
81 defined as

$$P \equiv K_{ow} \equiv \frac{[\text{neutral solute}]_{\text{oct}}}{[\text{neutral solute}]_{\text{wat}}} \quad (1)$$

¹SAMPL6 was originally announced as featuring a log D prediction challenge, but there were difficulties in the collection of experimental data. The original plan was to measure log P^0 , log P^{-1} , and log P^{+1} and calculate log D values at the experimental pH using these values. However, we were able to measure the partition coefficients of neutral species (log P^0) much more reliably than ionic species with potentiometric log P method of Sirius T3, as elaborated further below.

82 This quantity is often written in its \log_{10} form, which we denote here as $\log P$,

$$\log P = \log_{10} K_{ow} = \log_{10} \frac{[\text{neutral solute}]_{\text{oct}}}{[\text{neutral solute}]_{\text{wat}}} \quad (2)$$

83 However, ionic species can also partition between phases [30–32]. The partition coefficients of ionic species is calculated
84 using the same equation, e.g. P^{+1} refers to the partition equilibrium of +1 charge state of a molecule. Based on the experimental
85 measurement method this value may be defined for a single tautomer or may involve multiple tautomers.

$$\log P^{ion} = \log_{10} \frac{[\text{ionic solute}]_{\text{oct}}}{[\text{ionic solute}]_{\text{wat}}} \quad (3)$$

86 A closely related concept is that of the distribution coefficient (D_{ow} , often written in \log_{10} form as $\log D$) which should not be
87 confused with $\log P$. $\log D$ is the logarithm of the sum of *all* species (both neutral and ionized) concentrations in the organic
88 phase divided by the sum of neutral and ionic species concentrations in aqueous phase. Both octanol-water $\log P$ and $\log D$
89 values are frequently used as lipophilicity estimates [22]. However, while $\log D$ is pH-dependent, $\log P$ is independent of the pH
90 of the aqueous phase. As $\log P$ is defined as the partition coefficient of neutral species, it would include all neutral tautomer
91 populations if a compound can tautomerize.

92 The gold standard of partition coefficient measurement experimentation is the shake-flask method, according to the Organiza-
93 tion for Economic Cooperation and Development (OECD) [33]. Methods developed as experimental refinements on the shake-flask
94 method are high-throughput microscale shake flask [34, 35] and slow stirring methods [36]. Other direct methods for $\log P$ or
95 $\log D$ determination include dialysis chamber-based methods [37], micellar electrokinetic capillary chromatography [38, 39], and
96 counter-current chromatography [39]. An indirect experimental method that is widely used—despite being less reliable—is $\log P$
97 estimation based on reversed-phase high-performance liquid chromatography (HPLC) retention times [40–44]. The measurement
98 principle for all of these methods is the measurement of $\log D$ —the equilibrium distribution coefficient for both neutral and
99 ionized species—in a pH-dependent manner. As a result, in order to measure $\log P$ with these methods it is necessary to conduct
100 the $\log D$ measurements at a pH where the analyte is completely un-ionized. At a pH where the analyte is at a neutral state,
101 $\log P$ is *equal* to $\log D$; however, accurately predicting or measuring the equilibrium ionization constant (pK_a) of a substance is a
102 prerequisite. Here in this study, however, we pursued an alternate approach for experimental determination of $\log P$, which is
103 potentiometric measurements.

104 Potentiometric measurement of $\log P$ with the Sirius T3

105 The potentiometric $\log P$ measurement method determines $\log P$ values directly using potentiometric titrations in an immiscible
106 biphasic system [45, 46]. The shift of apparent pK_a values when the aqueous phase is in contact with the octanol phase is used to
107 estimate $\log P$ values. Experimental $\log P$ values presented in this study were collected using this potentiometric method, and
108 they refer to the partition coefficient of the neutral species.

109 The potentiometric $\log P$ measurement method used by the Sirius T3 instrument (Pion) [46–51] is based on determination
110 of the partition profile directly from acid-base titrations in a dual-phase water-partition solvent system consisting of two liquid
111 phases in contact (Fig. 1). In this method, multiple potentiometric acid-base titrations are performed in the aqueous phase at
112 various equilibrium volumetric ratios of octanol and water to observe the ionization and partitioning equilibrium behavior of the
113 analyte. As the relative volume ratio of octanol to water changes, a shift in apparent pK_a (p_oK_a) is observed due to partitioning
114 of neutral and ionic species—which have distinct octanol-water partitioning equilibria—into the octanol-rich phase. Equations
115 describing this coupled partitioning and ionization equilibria are then solved to determine the $\log P$ of the neutral and ionic
116 species. To use this method, aqueous pK_a value(s) must be known, and analytes must be fully water soluble at the highest
117 concentration they reach during the titrations throughout the entire range of pH titration selected for the potentiometric $\log P$
118 measurement protocol. The largest pH range selected for titration can be pH 2–12 and the minimum range should include ± 2 pH
119 units around the pK_a and p_oK_a .

120 When an ionizable substance is titrated in a two-phase system, the apparent pK_a —here, denoted p_oK_a —observed in the
121 titration shifts due to differential partitioning of neutral and ionized species into the nonaqueous phase. The p_oK_a value is the
122 apparent pK_a in the presence of partition solvent octanol. Its shift is dependent on the volumetric ratio of the water and octanol
123 phases. The p_oK_a value increases with increasing partition solvent volume for monoprotic acids and decreases with monoprotic
124 bases. The shift in p_oK_a is directly proportional to the $\log P$ of the compound and the ratio of octanol to water. For a monoprotic
125 acid or base, the partition coefficient of neutral (P^0) and ionic species (P^{-1} , P^{+1}) relates to pK_a and p_oK_a as [50],

$$\text{monoprotic acid : } P^0 = \frac{10^{(p_oK_a - pK_a)} - 1}{R} ; P^{-1} = \frac{10^{-(p_oK_a - pK_a)} - 1}{R} \quad (4)$$

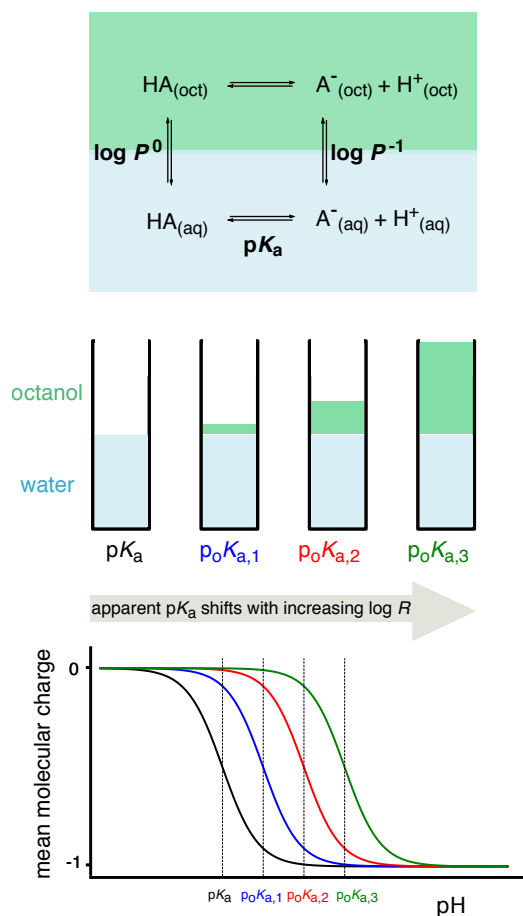


Figure 1. Potentiometric $\log P$ measurements are based on a model of ionization and partitioning equilibria [50]. Measurements of the pK_a and apparent pK_a (p_oK_a) at three octanol-water volumetric ratios ($\log R$) are performed to estimate the partition coefficients of neutral and ionized species, $\log P^0$ and $\log P^{-1}$, respectively. An ionization and partitioning equilibria model, along with estimated potentiometric titration curves, are shown for a monoprotic acid in this figure.

126

$$\text{monoprotic base : } P^O = \frac{10^{-(pO K_a - pK_a)} - 1}{R} ; P^{+1} = \frac{10^{(pO K_a - pK_a)} - 1}{R} \quad (5)$$

127 Here, R is the volume ratio of nonaqueous phase (V_{nonaq}) to aqueous phase (V_{aq}),

$$R \equiv \frac{V_{\text{nonaq}}}{V_{\text{aq}}} \quad (6)$$

128 2 Methods

129 2.1 Compound selection and procurement

130 For the SAMPL6 Part II log P Challenge, we attempted to collect log P measurements for the entire set of 24 kinase inhibitor
131 fragment-like compounds selected for the SAMPL6 pK_a Challenge [29, 52]. Details of compound selection criteria for the
132 SAMPL6 pK_a set—driven in large part by cheminformatics filtering for experimental tractability and rapid, inexpensive compound
133 procurement—can be found in the SAMPL6 pK_a experimental data collection paper [29]. Compounds with publicly available
134 experimental log P measurements were excluded by checking the following sources: DrugBank [53], ChemSpider [54], NCI Open
135 Database August 2006 release [55], Enhanced NCI Database Browser [56], and PubChem [57]. However, not all molecules selected
136 for SAMPL6 were suitable for log P measurements using the Sirius T3, due to various reasons such as low solubility, apparent pK_a
137 value shifting out of experimental range, or log P values out of experimental range limited by the sample vial. These limitations
138 are explained in more detail in the Discussion section. Only 11 small molecules proved to be suitable for potentiometric log P
139 measurements.

140 Molecule IDs assigned to these compounds for the SAMPL6 pK_a Challenge were preserved in the SAMPL6 Part II log P
141 Challenge. A list of SAMPL6 log P Challenge small molecules, SMILES, and molecule IDs can be found in Table 1. Counterions,
142 where present in solid formulations (see "Potentiometric log P measurements" section below), were included in SMILES for the
143 sake of completeness, although no significant effect is expected from the presence of chloride counterions as experiments were
144 conducted using KCl to maintain constant ionic strength. Procurement details for all compounds in the SAMPL6 log P Challenge
145 compounds are presented in Table S1.

146 2.2 Potentiometric log P measurements

147 Experimental octanol-water log P values of neutral species were collected using potentiometric log P (pH-metric log P) measure-
148 ments [50] at 25.0 ± 0.5 °C and constant ionic strength (0.15 M KCl). Aqueous pK_a values are required for log P determination with
149 the Sirius T3, and were previously determined for all compounds in this set [29] using UV-metric pK_a measurements [58, 59] with
150 the same instrument.

151 Three independent replicates were performed for each log P measurement using 1-octanol and water biphasic systems at
152 25.0 °C, starting with solid material. General guidance of according to the instrument manual suggests optimal analyte mass
153 should be in the range of 1–10 mg. "Sample weight" is the terminology used to describe analyte mass in Sirius T3 manuals,
154 software, and reports. Due to solubility limitations of the SAMPL6 compounds, we tried to use analyte masses less than 3 mg.
155 There was not much flexibility to adjust aqueous phase volume, since this is limited by the minimum volume required for the pH
156 probe (1.4–1.5 mL) and the volume that must be spared for the octanol phase in the sample vial. Therefore, we adjusted analyte
157 mass instead of aqueous phase volume when reducing sample concentration was necessary to achieve solubility.

158 For molecules with low solubility, target analyte mass was reduced, but not below a minimum of 1 mg. Samples were
159 prepared by weighing 1–3 mg of analyte in solid powder form into Sirius T3 analysis vials using a Sartorius Analytical Balance
160 (Model: ME235P) equipped with an antistatic ionizer. It was difficult to transfer powder compounds to achieve target masses
161 in 1–3 mg range exactly. Instead, we opted to weigh out approximate target mass ($\pm 40\%$ of the target mass was considered
162 acceptable) and record the resulting sample mass. For instance, when aiming for 1 mg of compound, if 1.29 mg of compound
163 was transferred to the balance, that was recorded as analyte mass and 1.29 mg was provided in to the Sirius T3 software for
164 analysis. Reporting accurate analyte mass was important since analyte mass and purity are part of the Sirius T3 refinement
165 model, although the analysis software doesn't accept analyte purity as an input. Analyte purity ("sample concentration factor"
166 according to Sirius T3) is estimated from the refinement model fit to experimental data given the reported analyte mass by the
167 user. The remaining steps in sample preparation were performed by the automated titrator: addition of ionic-strength adjusted
168 (ISA) water (typically 1.5 mL) and partition solvent (ISA water-saturated octanol), mixing, sonication, and titration with acid (0.5 M
169 KCl) and base (0.5 M KOH) solutions targeting steps of 0.2 pH units. ISA water is 0.15 M KCl solution which was used to keep ionic
170 strength constant during the experiment. ISA water was prepared by dissolving KCl salt in distilled water.

171 ISA water-saturated octanol was prepared by mixing 500 mL 1-octanol (Fisher Chemical, cat no A402-500, lot no 168525)
172 with 26.3 mL ISA water (targeting 5% ISA water-octanol mixture by volume) and letting the mixture phases separate before
173 attaching it to the automated titrator. Titrations were performed under argon flow on the liquid surface to minimize carbon
174 dioxide absorption from the air.

175 In some cases, to help with kinetic solubility issues of the analytes, solid samples were predosed manually with 80–100 μL ISA
176 water-saturated octanol prior to the addition of ISA water and partition solvent—these are noted in Table 1. Predosed volumes
177 were provided to the analysis software as an input and were accounted for in the total octanol volume calculation. Whenever
178 mean molecular charge vs pH plots showed experimental data points that deviated from the expected sigmoidal curve shape
179 (oscillatory shape or steeper descent), we suspected solubility problems and attempted to prevent them by predosing octanol,
180 which can only help the cases in which the solubility issue is a kinetic and not an equilibrium solubility issue. The only way to
181 alleviate an equilibrium solubility issue entirely is to lower the analyte concentration by starting the experiment with a smaller
182 analyte mass.

183 For each replicate log P measurement, three sequential automated acid-base titrations were performed in the same vial at
184 three different volume ratios of octanol and water, using 0.5 M KOH and HCl solutions as titrants while monitoring pH with a pH
185 electrode (Ag/AgCl double-junction reference electrode). Additional volumes of octanol were dispensed before each titration to
186 achieve target octanol-water ratios. The sequence of three octanol-water ratios were determined using predicted log R profiles
187 (apparent $\text{p}K_a$ shift vs \log_{10} of the volumetric ratios of partition solvents, as shown in Fig. 2C,D) or experimental log R profile if a
188 previous iteration of the experiment is available during protocol optimization, with the goal of selecting three volumes that will
189 maximize the $|\text{p}K_a - \text{p}_oK_a|$ values between each titration. Experiments were designed so that maximum separation of p_oK_a values
190 can be achieved while the total liquid volume in the analysis vial did not exceed 3 mL by the end of the third titration.

191 Two Sirius T3 software programs were used to execute measurement protocols (Sirius T3 Control v1.1.3.0) and analyze
192 experiments (Sirius T3 Refine v1.1.3.0). The Sirius T3 Refine software has the capability of fitting partitioning and ionization
193 equilibrium models to potentiometric data collected from a biphasic system to estimate log P values. The starting point for the
194 model fit is simulated titration curves constructed using aqueous $\text{p}K_a$ values (using prior $\text{p}K_a$ measurements, here taken from
195 [29]), predicted log P values, input analyte mass, and volumes of aqueous and organic phases dispensed to prepare the sample.
196 Collected experimental measurements (pH vs dispensed volume of acid and base solutions) were used to refine the model
197 parameters (log P of neutral species, log P of ionic species, analyte concentration factor, carbonate content, acidity error) to
198 determine the log P values of neutral species and ions [48]. Potentiometric log P measurements have the potential to determine
199 the partition coefficients of the ionic species (log P^1) in addition to log P of the neutral species (log P^0). It was, however, very
200 challenging to design experiments to capture log P values of the ionic species due to volumetric limitations of the glass analysis
201 vial and measurable pH range. Therefore, while optimizing experimental protocols, we prioritized the accuracy for only log P of
202 the neutral species. Experimental protocols were optimized iteratively by adjusting octanol-water ratios, analyte concentration,
203 and pH interval of the titration.

204 A partitioning and ionization equilibrium model [48] was fit to potentiometric measurements to estimate log P values of
205 the neutral species and also the charged species, as implemented in Sirius T3 Refine Software. Experiments were optimized to
206 determine log P of neutral species with good precision. log P estimates of charged species had high variance between replicate
207 experiments performed in this study and were judged to be unreliable. Optimizing experiments further to be able to capture
208 log P values of ionic species accurately would require larger log R values, which was limited by sample vial volume. Therefore, we
209 decided not to pursue experimental data collection for ionic partition coefficients further.

210 2.3 Reporting uncertainty of log P measurements

211 Experimental uncertainties of log P measurements were reported as the standard error of the mean (SEM) of three or four
212 replicates. The standard error of the mean (SEM) was estimated as

$$\text{SEM} = \frac{\sigma}{\sqrt{N}} \quad ; \quad \sigma = \sqrt{\frac{1}{N-1} \sum_{i=1}^N (x_i - \mu)^2} \quad ; \quad \mu = \frac{1}{N} \sum_{i=1}^N x_i \quad (7)$$

213 where σ denotes the unbiased sample estimator for the true standard deviation and μ denotes the sample mean. x_i are
214 observations and N is the number of observations.

215 The SEM calculated from independent replicate experiments as above was found to be larger than non-linear fit error reported
216 by the Sirius T3 Refine Software from potentiometric log P model fit of a single experiment, thus leading us to believe that running

217 replicate measurements and reporting mean and SEM of log P measurements better captured all sources of experimental
218 uncertainty. We caution, however, that the statistical error estimated from three replicates is only determined to an order of
219 magnitude [60].

220 2.4 Quality control of analytes

221 Purities of all SAMPL6 pK_a Challenge compounds—a subset of which formed the log P set used here—were determined by LC-MS
222 and reported elsewhere [29]. The same lots of compounds were used for pK_a and log P measurements. LC-MS assessment
223 showed that the 11 compounds reported in this study have a minimum of 96.5% purity and matching molecular weight to
224 supplier reported values (Table S1).

225 When questions were raised about the accuracy of log P measurements for SM13 by a participant of SAMPL6 log P Challenge,
226 we had additional quality control experiments performed to confirm the compound identity of SM13. LC-MS and NMR data were
227 fully consistent with the structure of SM13 as originally provided (Figure S1, S2). High-Resolution Mass Spectrometry (HRMS) data
228 was acquired using an Agilent 6560 Q-ToF by +ESI. NMR data were acquired for the sample dissolved in pyridine- d_5 . 1H , DQF-COSY,
229 and ROESY spectra were acquired using a 600 MHz Bruker AVANCE III HD spectrometer equipped with a liquid nitrogen-cooled
230 broadband Prodigy probe. Chemical shifts were assigned to validate the structure of SM13.

231 3 Results

232 In this study, we attempted to use the potentiometric log P measurement method of the Sirius T3 to measure log P values for
233 24 compounds of the SAMPL6 pK_a Challenge set. For 13 of the selected compounds, experimental constraints set by solubility,
234 lipophilicity, pK_a properties of the analytes, and experiment analysis volume limitations of the Sirius T3 instrument resulted in an
235 inability to achieve reliable log P measurements suitable for the blind challenge (Table S4). For example, SM24 has a basic pK_a of
236 2.60 and we could not optimize log P measurement protocol because in the presence of octanol phase apparent pK_a was shifting
237 beyond the measurable pH range of the Sirius T3. On the other hand SM03 log P could not be measured with potentiometric
238 method due to its low aqueous solubility. Only 11 of 24 compounds from the SAMPL6 pK_a Challenge set were found to be suitable
239 for potentiometric log P measurements with the Sirius T3. The resulting challenge dataset presented here has a log P range
240 of 1.95–4.09. Six of these represent the 4-amino quinazoline scaffold (SM02, SM04, SM07, SM09, SM12, SM13). There are two
241 benzimidazoles (SM14, SM15), one pyrazolo[3,4- d]pyrimidine (SM11), one pyridine (SM16), and one 2-oxoquinoline (SM08) (Fig. 3).
242 The mean and SEM of replicate log P measurements, SAMPL6 compound IDs (SMXX), and SMILES identifiers of these compounds
243 are presented in Table 1. In all cases, the SEM of the log P measurements ranged between 0.01–0.07 \log_{10} units.

244 Results of independent replicate measurements are presented in Table S2. Preparation of each replicate sample started
245 from weighing dry powder of the same analyte lot. The log P estimates from potentiometric titrations were evaluated using the
246 partitioning and ionization equilibrium model as implemented in the Sirius T3 Refine software, which produces log P estimates for
247 both neutral and ionic species. We observed that log P values of neutral species were highly reproducible, while variance of log P
248 of ionized species between replicate experiments was high. It was also not possible to measure log P values of the ionized species
249 reliably as doing so would require sampling higher log R values. Since it was prohibitively difficult to optimize experimental
250 protocols to capture partitioning of ionic species accurately, we optimized the experiments to prioritize accurate measurement of
251 neutral species log P (log P^0) and constructed the blind computational prediction challenge based on log P^0 values.

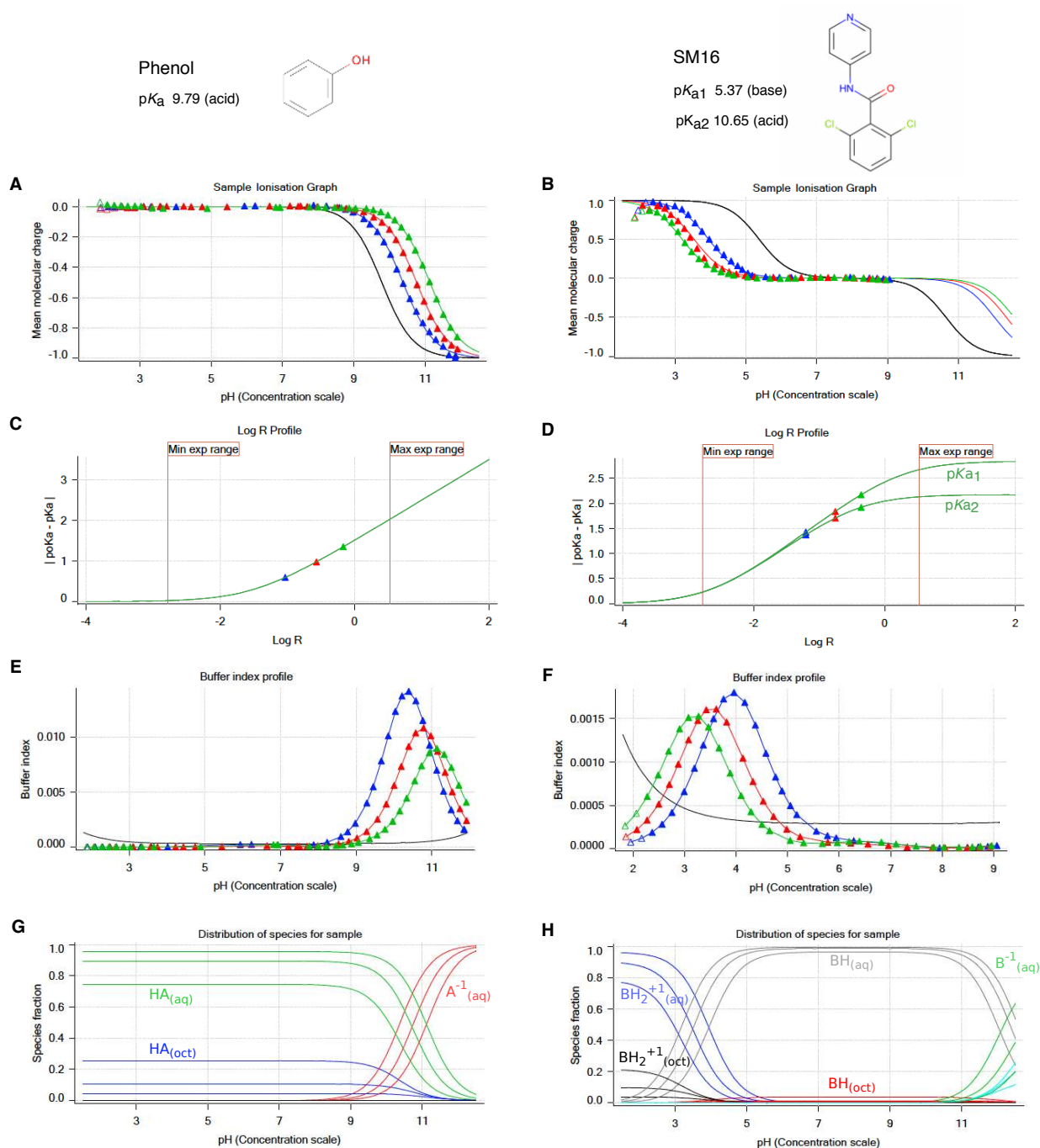


Figure 2. Illustrative potentiometric log *P* measurements of phenol (monoprotic, acid, log *P* 1.49) and SM16 (diprotic, amphoteric, log *P* 2.62) with the Sirius T3. Triangles represent experimental data points collected during the octanol-ISA water titrations and solid lines represent the ionization and partitioning model fit to the data. **A, B:** Computed mean molecular charge vs pH. Mean molecular charge is calculated based on experimental pK_a values and types (acid or base type) of the analyte. The black line is the model titration curve in aqueous media and based on the aqueous pK_a. Blue, red, and green triangles represent three sequential titrations with increasing log *R* (increasing octanol) that show shifted p_oK_a values. The inflection point of titration curves indicates the pK_a or p_oK_a, though these values are obtained by a global fit. For titration of acidic species, partitioning into the octanol phase increases the observed p_oK_a. In the titration of the basic pK_a of SM16, increasing log *R* causes a decrease in p_oK_a. The pH range of the experiment was determined such that only the titration of basic pK_a was captured (molecular charge between +1 and 0). **C, D:** log *R* profiles show a shift in p_oK_a with respect to increasing relative octanol volume. These plots aid in the design of the experiment and selection of optimal octanol volumes that aim to maximize separation between p_oK_a values for better model fit within experimental limitations (pH and analysis vial volume). **E, F:** Buffer index profiles show buffering capacity observed in three titrations with increasing log *R* (blue to green). The black line is the intrinsic buffering capacity of water. For an accurate potentiometric measurement, buffering capacity signal of the analyte must be above the buffering capacity of water. As octanol volume increases, the concentration of the analyte in aqueous phase, and thus buffering capacity, decreases. **G, H:** Predicted relative populations of ionization states in octanol and water phases as a function of pH, based on the equilibrium model fit to experimental data.

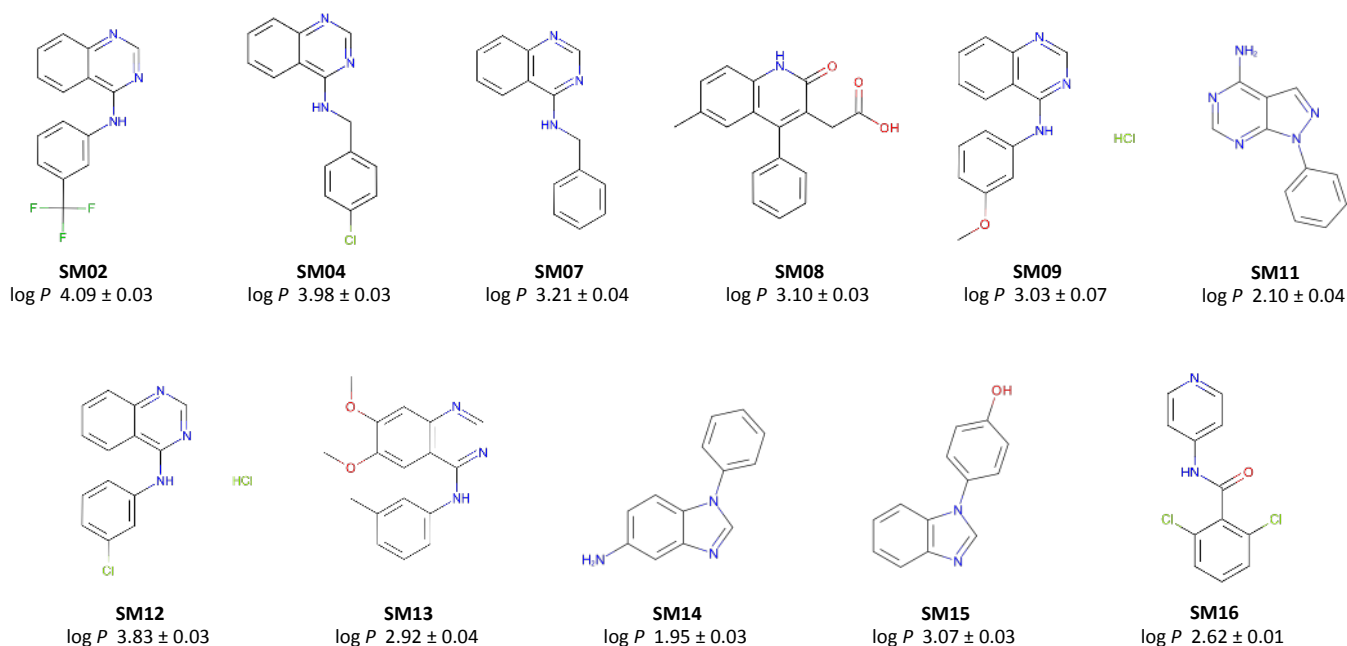


Figure 3. Molecules included in the SAMPL6 Part II log P Challenge set. Reliable experimental potentiometric log *P* measurements were collected for the 11 molecules depicted here. Reported uncertainties are expressed as the standard error of the mean (SEM) of replicate measurements. Molecules are depicted using OpenEye OEDepict Tool [61]. Canonical isomeric SMILES strings of all compounds are given in Table 1, and replicate log *P* measurements can be found in Table S2.

Table 1. Experimental log *P* measurements for the SAMPL6 Part II log P Challenge. Potentiometric log *P* measurements were performed with the Sirius T3 in ISA water. Triplicate measurements were performed at 25.0 ± 0.5 and in the presence of 150 mM KCl to control ionic strength. log *P* values are reported as mean ± SEM of at least three independent replicates. log *P* values of independent replicate measurements are presented in Table S2. A computer readable form of this table can be found in the SI documents bundle (*logP_experimental_values.csv*).

Molecule ID	N ¹	log <i>P</i> (mean ± SEM)	Assay Type	Isomeric SMILES
SM02	3	4.09 ± 0.03	potentiometric octanol log <i>P</i>	<chem>c1ccc2c(c1)c(ncn2)Nc3cccc(c3)C(F)(F)F</chem>
SM04	3	3.98 ± 0.03	potentiometric octanol log <i>P</i>	<chem>c1ccc2c(c1)c(ncn2)NCc3ccc(cc3)Cl</chem>
SM07	3	3.21 ± 0.04	potentiometric octanol log <i>P</i>	<chem>c1ccc(cc1)CNc2c3cccc3ncn2</chem>
SM08	3	3.10 ± 0.03	potentiometric octanol log <i>P</i> ²	<chem>Cc1ccc2c(c1)c(c(=O)[nH]2)CC(=O)O)c3cccc3</chem>
SM09	3	3.03 ± 0.07	potentiometric octanol log <i>P</i>	<chem>COc1cccc(c1)Nc2c3cccc3ncn2.Cl</chem>
SM11	4	2.10 ± 0.04	potentiometric octanol log <i>P</i>	<chem>c1ccc(cc1)n2c3c(cn2)c(ncn3)N</chem>
SM12	4	3.83 ± 0.03	potentiometric octanol log <i>P</i>	<chem>c1ccc2c(c1)c(ncn2)Nc3cccc(c3)Cl.Cl</chem>
SM13	3	2.92 ± 0.04	potentiometric octanol log <i>P</i> ³	<chem>Cc1cccc(c1)Nc2c3cc(c(cc3ncn2)OC)OC</chem>
SM14	4	1.95 ± 0.03	potentiometric octanol log <i>P</i>	<chem>c1ccc(cc1)n2cnc3c2ccc(c3)N</chem>
SM15	3	3.07 ± 0.03	potentiometric octanol log <i>P</i>	<chem>c1ccc2c(c1)ncn2c3ccc(cc3)O</chem>
SM16	3	2.62 ± 0.01	potentiometric octanol log <i>P</i> ³	<chem>c1cc(c(c(c1)Cl)C(=O)Nc2ccncc2)Cl</chem>

¹ Number of replicates

² Sample predosed with 80 μL octanol to address kinetic solubility issues

³ Sample predosed with 100 μL octanol to address kinetic solubility issues

253 4.1 Dynamic range of log *P* measurements and solubility limitations

254 We attempted to measure the log *P* for all 24 SAMPL6 pK_a Challenge compounds, but the Sirius T3 potentiometric log *P*
255 measurement method was able to provide reliable measurements for only a subset of 11 molecules which were included in
256 the blind challenge. We only included molecules that yielded reliable, precise log *P* measurements in the computational blind
257 challenge.

258 A number of factors restricted the ability to perform reliable log *P* measurements and led to elimination of some compounds
259 from the initial set of 24: low water solubility within the pH range of the titration, the limited volume capacity of the glass sample
260 vial which limits the maximum achievable octanol:water ratio, the octanol-dependent p_oK_a values shifting outside the measurable
261 pH range of 2–12 (especially high acidic pK_a s and low basic pK_a s). If an analyte does not suffer from the issues mentioned above,
262 dynamic range of this log *P* measurement method is limited by smallest (related to dispensing accuracy and evaporation rate)
263 and largest octanol volumes (related to analysis vial volume) that can be dispensed.

264 4.2 Optimizing experimental protocols for each compound

265 For the set of compounds in SAMPL6 Challenge, we observed that the Sirius T3 potentiometric log *P* measurement experiments
266 were in practice very low throughput because of the necessary iterative protocol optimization for each compound. The parameters
267 determining a potentiometric log *P* experiment are: mass of analyte, initial volume of ISA water, three target volumes of octanol
268 for sequential titrations with increasing log *R*, and pH range of the pH titration. Factors that were considered in this optimization
269 and limitations of choice are discussed below.

270 4.2.1 Optimizing the sequence of octanol-water volumetric ratios and range of pH titration

271 To obtain reliable and precise log *P* estimates from experimental data, it is recommended to fit the ionization and partitioning
272 equilibrium model to at least three potentiometric titrations with well separated p_oK_a values (Figure 2A, B). log *P* values can also
273 be estimated from two potentiometric titrations, but not as accurately. p_oK_a values of sequential titrations need to be at least
274 0.3 pK_a units separated from one another and from the aqueous pK_a . To achieve this, selecting an optimal set of octanol-water
275 volumetric ratios is key.

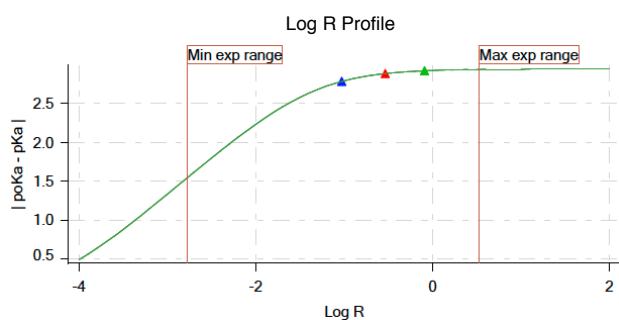
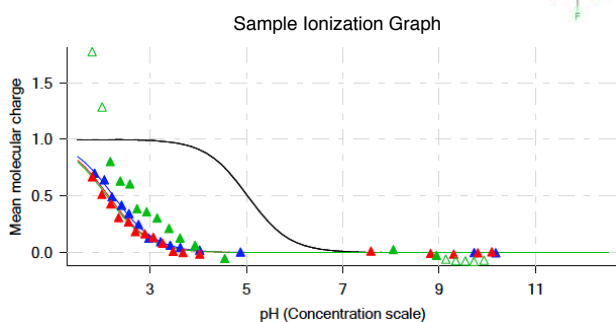
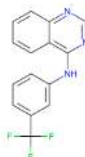
276 It is logical to target the largest difference in octanol volumes, but the minimum volume of aqueous phase that provides
277 enough depth for the pH probe (1.4 mL) and maximum analysis vial volume (3 mL) result in only 1.6 mL of available volume for
278 the octanol phase, limiting the maximum octanol:water volume ratio *R* to ~ 1.1. Typically, one would pick octanol volumes for
279 each of three sequential titrations that maximize the difference in p_oK_a by maximizing the difference in log *R* values as much as
280 possible considering the other experimental constraints. Simulated log *R* profiles based on predicted log *P* and experimental pK_a
281 values provide guidance in the selection of octanol volumes (Fig. 2C, D). These plots show how much $|pK_a - p_oK_a|$ difference can
282 be gained with respect to a change in log *R*, based on the titration and ionization propensity of each molecule, but they are only
283 as useful as the accuracy of log *P* prediction. For that reason, potentiometric log *P* measurements needs to be optimized with an
284 iterative process where the first experimental protocol is designed using predicted log *P* and experimental pK_a of the analyte.
285 Based on the p_oK_a shifts and quality of titration curves observed, a second experiment is designed to improve p_oK_a shifts by
286 adjusting the octanol volumes after consulting the log *R* profile and using the estimated log *P* from the previous experiment as a
287 guide. Sometimes 3 or 4 iterations were necessary to reach an optimal protocol that results in a good fit between predicted and
288 experimental titration curves and produces reproducible log *P* estimates. An example protocol optimization for SM02 guided by
289 log *R* values is shown in Fig. 4.

290 While maximizing the difference in p_oK_a values from each other and from the aqueous pK_a is desirable, sometimes it is
291 necessary to reduce the octanol volume to limit the shift in p_oK_a so that it remains within a measurable range. This would be
292 necessary when the aqueous pK_a is a weak acid ($pK_a > 9$) or weak base ($pK_a < 5$), since the presence of the octanol phase causes
293 p_oK_a shifts towards higher and lower values, respectively, approaching the limit of the measurable pH range of the instrument.
294 Measurable pH range is mainly limited by the acid and base strength of titration solutions against the increasing buffering capacity
295 of water at pH values below 2 and above 12. It is also important to mention that even if the p_oK_a value itself is within the stated
296 measurement range of 2–12, if a large portion of the titration curve is beyond limits (i.e., saturation of fractional population on
297 both sides of the p_oK_a), then the experimental titration curve may not be fit to the model titration curve exactly and p_oK_a cannot
298 be determined as precisely. When the dynamic part of the titration curve ($p_oK_a \pm 2$) shifts outside of the measureable pH range, it
299 reduces the confidence in p_oK_a estimates of the fit. Therefore, p_oK_a values should ideally be at least ± 1 unit, and preferably ± 2
300 units away from the limits of pH measurement with this instrument, which can be extended to pH 1 and 13 at most. For this
301 reason, it is easier to optimize log *P* experiments for monoprotic molecules which have acidic pK_a s between 3–10 and basic pK_a s

A Before optimization for log *R*

Sample weight: 1.87 mg
 ISA water volume: 1.50 mL
 Additional octanol volume (Titration 1): 0.150 mL
 Additional octanol volume (Titration 2): 0.350 mL
 Additional octanol volume (Titration 3): 1.000 mL

SM02



B After optimization for log *R*

Sample weight: 1.87 mg
 ISA water volume: 1.50 mL
 Additional octanol volume (Titration 1): 0.020 mL
 Additional octanol volume (Titration 2): 0.025 mL
 Additional octanol volume (Titration 3): 0.100 mL

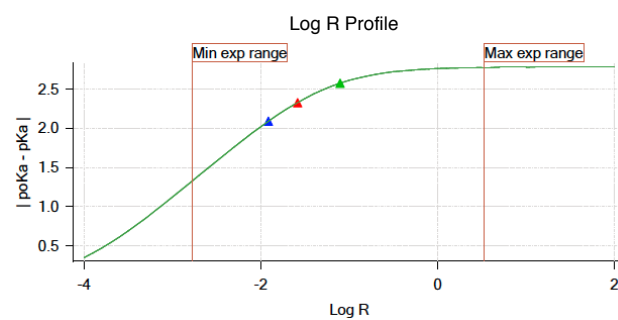
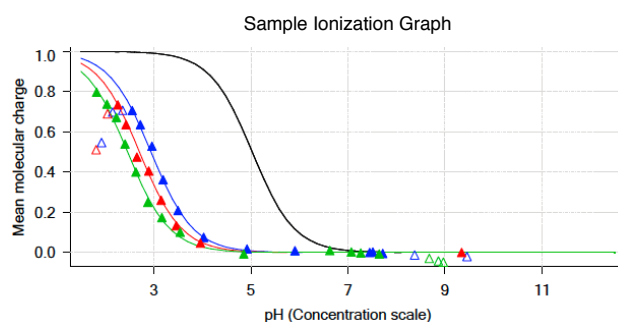


Figure 4. Potentiometric log *P* protocol optimization of SM02 based on log *R*. Experimental results of initial trial (A) and optimized protocol (B) are shown for SM02. log *R* profile before optimization (A lower panel) shows insufficient apparent pK_a shift due to poor choice of octanol-water volume ratios. This experiment led to log *P* and log P^{+1} estimates of 4.32 and 1.38. For a good measurement, triangles that indicate $|pK_a - p_oK_a|$ of each titration in log *R* profiles must fall on the slope region of the log *R* profile instead of the plateau region. Adjusting log *R* by decreasing octanol volumes in each titration led to a better experiment with distinct titration curves and well separated p_oK_a values (B). log *P* and log P^{+1} were measured as 4.10 and 1.32 with the optimized protocol. Once we achieved optimization of potentiometric log *P* protocol, triplicate measurements were collected using the same protocol.

302 between 4–11. Some molecules in the SAMPL6 set which were not suitable for potentiometric log P measurements because of
303 this criteria were: SM01, SM17, SM18, SM19, and SM24 (Table S4).

304 4.2.2 Sample preparation considerations and determination of appropriate starting concentration

305 Sample preparation starts with the weighing of solid powder material to analysis vials. How much analyte to use is another
306 important decision that requires optimization. General guidance according to the Sirius T3 manual is to use 1–10 mg, and the
307 aqueous phase volume is typically adjusted to the minimum volume (1.4–1.5 mL). The buffering capacity and compound solubility
308 are the two factors that guide lower and higher limits of suitable analyte concentration. The Sirius T3 produces buffer index vs
309 pH plots (Fig. 2E, D) which provide guidance on how much analyte is needed for sufficient potentiometric signal. To guide the
310 first experiment, these plots can be simulated based on analyte mass, experimental pK_a , predicted log P , and selected octanol
311 volumes. In further iterations of experiments, the buffer index profiles of the previous experiment guides the decisions about how
312 to optimize the protocol. On the other hand, aqueous solubility limits the maximum concentration of the analyte in the aqueous
313 phase. Moreover, since the experimental methodology depends on measuring the p_oK_a shift during pH titrations as species
314 partition into the nonaqueous phase, the analyte must stay in solution over the titrated pH range for the entire experiment, as
315 the presence of an insoluble phase represents another reservoir for compound partitioning that would invalidate the coupled
316 ionization-and-partitioning model used to compute the log P . The pH titration range is adjusted to capture a sufficient region
317 below and above the p_oK_a to ensure ionization states with lower solubility are also visited (neutral and zwitterionic states).

318 For these compounds resembling fragments of kinase inhibitors –the compounds considered in the SAMPL6 pK_a Challenge [29]
319 and this study– this solubility criterion turned out to be very challenging to meet. A large portion of compounds in the SAMPL6
320 pK_a Challenge set were found to be insufficiently soluble for potentiometric log P experiments at some region of the pH range
321 that needs to be titrated during the experiment, more likely the pH region where the neutral population of analytes are prominent.
322 These compounds for which potentiometric log P measurement could not be optimized due to solubility limitations are listed in
323 Table S4. For other compounds, we had to try reducing the analyte sample quantity from 3 mg to 1 mg of compound to find
324 the optimum balance between ensuring the compound remained fully soluble and ensuring sufficiently high buffering capacity
325 signal. The rate of change of pH vs. volume of acid or base titrated in analyte solution must differ from the rate of pH change in
326 just water. This quantity is expressed as a buffering index in buffer index profiles generated by Sirius T3 (Fig. 2E,F), where a black
327 solid line describes the theoretical buffering capacity of water and colored triangles describe the experimental buffering capacity
328 of the analyte. For high quality measurements, reaching at least 0.001 buffer index at the maximum point of the titration (at pH
329 that equals p_oK_a) is recommended.

330 In our case, the exact solubility of compounds was not known prior to log P measurements. We had to evaluate precipitation
331 issues based on the distortion of mean molecular charge vs pH profiles (Fig. 2E, D) from ideal shape by adjusting starting
332 analyte masses until the distortions disappear. Distortions manifest as very steep drops or oscillations in relative ionization state
333 populations with respect to pH. An example is shown in Fig 5A Sample Ionization Graph. The turbidity indicator of Sirius T3 can
334 not be utilized for solubility detection during log P experiments since the presence of octanol causes turbidity in the aqueous
335 phase due to vigorous stirring during titrations. Predosing 80–100 μ L octanol before addition of ISA water, as well as sonication
336 and stirring after titrant addition, were also helpful for overcoming kinetic solubility problems. An example protocol optimization
337 for SM08 to overcome solubility problems is shown in Fig 5.

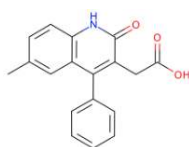
338 If possible, measuring solubility of compounds prior to potentiometric log P measurements can provide helpful information
339 for more efficient log P measurement protocol optimization. However, since solubility is pH-dependent, the lowest solubility
340 of the compound during the entire pH 2–12 range would be the information necessary to guide the experimental design. An
341 experiment for a compound with 400 g/mol molecular weight using the minimum analysis made of 1 mg and 1.5 mL of aqueous
342 phase corresponds to 1.67 mM. To be suitable for potentiometric log P measurements with the Sirius T3, at least 1.67 mM
343 aqueous solubility is necessary throughout the pH range of the analysis.

344 One way to increase the dynamic range of potentiometric log P measurement with the Sirius T3 is to increase the range of
345 log R that can be sampled by performing three different p_oK_a measurements in three different analysis vials instead of three
346 sequential titrations in one vial. But since log R is dependent on the cumulative octanol volume in sequential titrations, the
347 advantage of the single titration approach is not significant. The single titration approach can only allow a small additional volume
348 for octanol phase which would be used to dispense multiple acid and base stock solution volumes (~0.2 mL). We did not elect to
349 investigate this design because we did not want to introduce another source of error: the variance in sample mass between
350 measurements. Since the initial sample mass is an input parameter to the experimental model, using three different sample
351 masses would introduce effects coming from the inaccuracy of the analytical balance to log P estimates.

A Before optimizing for solubility

Sample weight: 1.08 mg
 Predose octanol volume: 0.025 mL
 ISA water volume: 1.50 mL
 Additional octanol volume (Titration 1): 0.025 mL
 Additional octanol volume (Titration 2): 0.040 mL
 Additional octanol volume (Titration 3): 0.500 mL

SM08



B After optimizing for solubility

Sample weight: 0.98 mg
 Predose octanol volume: 0.080 mL
 ISA water volume: 1.50 mL
 Additional octanol volume (Titration 1): 0.080 mL
 Additional octanol volume (Titration 2): 0.200 mL
 Additional octanol volume (Titration 3): 0.800 mL

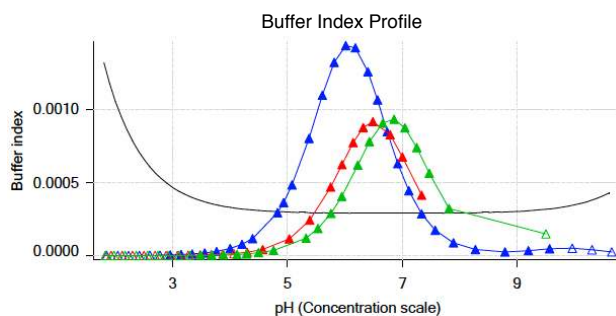
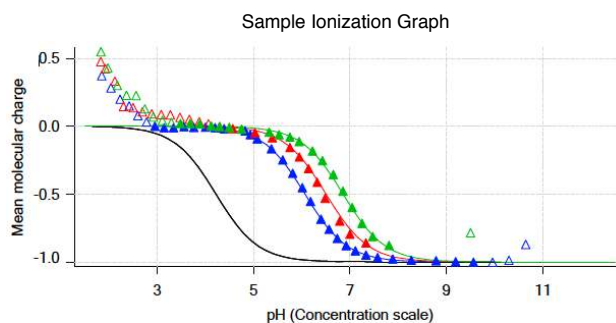
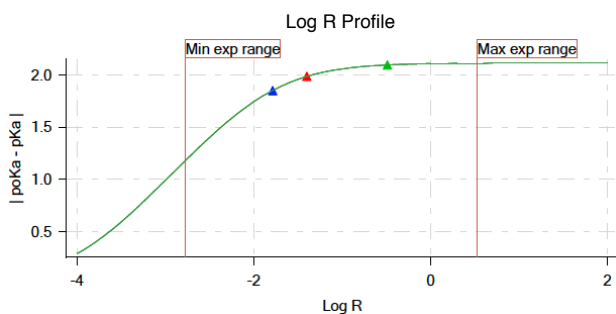
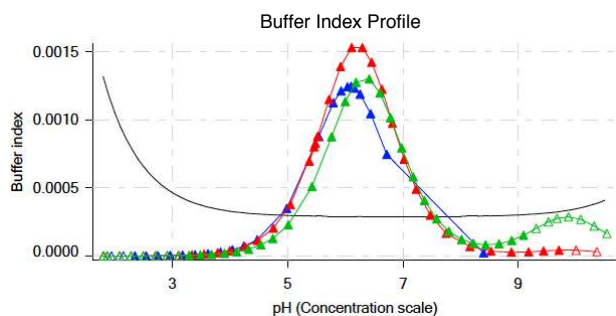
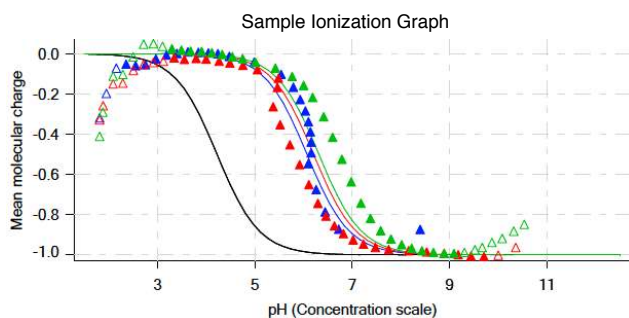


Figure 5. Potentiometric log P protocol optimization for SM08 to alleviate aqueous solubility problems. Experimental results of initial protocol (A) and the optimized protocol (B) are shown for SM08. Both first (blue) and second (red) titrations in Sample Ionization Graph before optimization (A lower panel) show deviation from expected sigmoidal shape which is an indication of an insoluble analyte. This experiment with solubility issues led to $\log P$ and $\log P^{+1}$ estimates of 3.97 and 1.86. To eliminate precipitation, we could not lower analyte mass below 1 mg. Instead we were able to optimize the experimental protocol by increasing the predosed octanol volume and increasing additional octanol volumes added in each titration. Predosing octanol helps only with kinetic solubility issues. Larger octanol volumes can help to improve the experiment when thermodynamic solubility is the limitation, by allowing larger amounts of analyte partitioning into the octanol phase and reducing the analyte concentration in aqueous phase. Additional octanol volumes were selected such that they would also improve log R profile of the measurement. With optimized protocol (B) we achieved sample ionization profiles without any precipitation effects. $\log P$ and $\log P^{+1}$ were measured as 3.16 and 0.23. Once we achieved optimization of potentiometric log P protocol, triplicate measurements were collected using the same protocol.

352 Another way to prepare analyte samples for Sirius T3 measurements is to start from DMSO stock solutions instead of dry
353 powder stocks. However, potentiometric measurements require 1–10 mg/mL analyte concentration in order to reach sufficient
354 buffering capacity. The required concentration of the DMSO stock solution would be quite high, and sometimes impossible due
355 to solubility limits in DMSO. Typical DMSO stock solution concentrations are 10 mM. For an analyte with 400 g/mol molecular
356 weight, the concentration of 10 mM DMSO stock solution corresponds to 4 mg/mL. In order to achieve the minimum required 1
357 mg/mL analyte solution for the Sirius T3 experiment, the aqueous phase would have to consist of 25% DMSO which would cause
358 significant cosolvent effects. On the other hand, achieving lower cosolvent presence, such as 2.5% DMSO, would require DMSO
359 stock solutions of 100 mM at which concentration the analyte may not be soluble. Presence of cosolvent at even low amounts
360 is undesirable due to the potential the effect on the log P measurements. Therefore, it is not recommended to perform these
361 experiments starting from DMSO stock solutions.

362 4.3 Reliable determination of log P values of ionized species was not possible

363 Although it is possible to use Sirius T3 potentiometric log P measurements to determine the partition coefficients of ionic species
364 as well, in practice, we were not able to achieve log P^1 estimates with low variance between experiments. The partitioning of
365 ionic species into the organic phase is typically much lower than that of the neutral species, and to capture this accurately by
366 measuring sufficiently large p_oK_a shifts, it would be necessary to use much larger octanol to water volumetric ratios R . The
367 Sirius T3 glass analyte vials can hold up to 3 mL, which limits the maximum achievable octanol to water volumetric ratio. Since at
368 least 1.4 mL must be devoted to the aqueous phase for the pH probe, this leaves only 1.6 mL for the octanol phase, producing a
369 maximum achievable $R \sim 1.1$. Another limitation was the measurable pH range. Since log P measurements rely on determining
370 well-separated p_oK_a values at different log R values to get a good model fit, the octanol to water volumetric ratio needs to be
371 selected such that p_oK_a values are well separated but not out of the measurable pH range (2–12).

372 To capture the partitioning of ionic species to the octanol layer reliably, experiments need to be set up with larger log R ratios
373 which is problematic if this causes p_oK_a to shift outside of the measurable pH range. Therefore, we designed the experiments
374 to capture only the partition coefficient of the neutral species (log P^0) accurately. The SAMPL6 log P Prediction Challenge was
375 constructed only on prediction of neutral species.

376 The lack of reliable determination of partition coefficient values of the ionic species (log P^{+1} or log P^{-1}) may be a source of
377 systematic error in the estimate of log P of the neutral species (log P^0). For hydrophobic compounds with negligible partitioning
378 of the ionic species into the octanol-rich phase (log P^{+1} , log $P^{-1} \leq 2$), log P^0 estimates would still be accurate even if ion partitioning
379 is not captured well. For compounds that may have higher levels of ionic partitioning, to minimize the impact of inaccurate
380 log P^{+1} or log P^{-1} experimental estimates on log P^0 measurements, we used ACD/Labs predicted log P^{+1} and log P^{-1} values as the
381 starting point for the refinement of the ionization and partitioning equilibrium model parameters (performed with Sirius T3
382 Refine Software).

383 4.4 Absence of zwitterions allowed accurate log P measurements of amphoteric molecules

384 Multiple publications point out discrepancies between log P values determined by the potentiometric method and the shake-flask
385 experiments for zwitterionic compounds [62, 63]. There are multiprotic compounds in the SAMPL6 dataset (SM14, SM15, and
386 SM16), but we believe these measurements were not affected by this problem because they are not zwitterionic. Zwitterionic
387 molecules have a zwitterion as the dominant neutral state in the pH region between the two pK_a s (a lower acidic pK_a and a higher
388 basic pK_a). SM14 has two basic pK_a s and is not found as a zwitterion at any pH between 2–12. SM15 and SM16 are amphoteric
389 compounds that possess both acidic and basic titratable groups, however, according to spectrophotometric pK_a measurements
390 in the presence of cosolvent their acidic pK_a values are higher than their basic pK_a values. This means the major neutral form of
391 these compound is the non-charged state, not a zwitterion. Spectrophotometric pK_a measurements with varying percentage of
392 methanol as cosolvent were performed with the Sirius T3 and included in supplementary documents. Acidic or basic character of
393 macroscopic pK_a values was assigned based on the slope of Yasuda-Shedlovsky plots.

394 In addition, quantum mechanics calculations [64] do not predict the presence of multiple tautomers of the neutral state at
395 significant populations for any of the molecules in the SAMPL6 log P Challenge set. Possible tautomers, such as the zwitterionic
396 state, are predicted to be much higher in energy and thus unlikely to play a significant role even if we considered a prediction
397 error margin for quantum mechanics-based calculations. Therefore, we do not think our potentiometric log P measurements are
398 influenced by presence of zwitterions or minor tautomeric forms.

399 4.5 Suggestions for future log *P* data collection

400 High quality datasets of experimental physicochemical property measurements are valuable for testing computational predictions.
401 Benchmarking and evaluation efforts like the SAMPL challenges benefit from large experimental datasets with diverse chemical
402 species. The quality of log *P* measurements collected with the Sirius T3 potentiometric method are satisfactory and comparable
403 to gold standard shake flask measurements [45, 49, 51]. The Sirius T3 potentiometric log *P* method requires aqueous pK_a s to be
404 measured experimentally ahead of time. The ability to obtain log *P* measurements of neutral and charged species separately,
405 instead of measuring pH dependent log *D*, is a unique advantage of the Sirius T3 approach compared to shake-flask or HPLC-based
406 methods where ionization effects are involved with partitioning behaviour. However, due to previously discussed limitations and
407 the necessity for extensive protocol optimization for each analyte, we are reluctant to suggest potentiometric log *P* measurements
408 with the Sirius T3 as a general and high-throughput method for future log *P* data collection unless significant resources and work
409 hours of a human expert can be dedicated to protocol optimization and data collection.

410 Informed selection of analytes can help improve the success of Sirius T3 experiments. For example, this approach is easier to
411 apply to highly soluble compounds (more than 1 mg/ml solubility in 0.15 M KCl through the entire range of pH titration range at
412 room temperature) with pK_a values in the midrange ($3 < \text{acidic } pK_a < 10$ and $4 < \text{basic } pK_a < 11$). There is no significant difference in
413 difficulty between the measurements of monoprotic vs multiprotic compounds, as long as one of the pK_a values of the multiprotic
414 compound is in the midrange. For determining the log *P* of neutral species, it is sufficient to collect potentiometric titration data
415 between the neutral state and the +1 or -1 charged states by titrating the pH region that captures the relevant p_0K_a values. It is
416 not necessary to capture the titration of a second pK_a (Fig. 2B).

417 Our opinion is that log *D* measurements at a buffered pH can be much more easily obtained in a higher throughput fashion
418 using miniaturized shake-flask measurements, such as those used in SAMPL5 log *D* Challenge experimental data collection [21].
419 To obtain log *P* values from experiments that were designed to measure log *D*s, it is necessary to measure the pK_a of compounds
420 (such as with the Sirius T3) and conduct log *D* measurements using a buffered aqueous phase at a pH that will ensure that
421 the analyte is completely in the neutral state. According to our experience, optimizing pK_a measurements with the Sirius T3 is
422 significantly easier than optimizing log *P* measurements, especially if a spectrophotometric (UV-metric) pK_a method can be used
423 instead of potentiometric, which is not an option for log *P* measurements.

424 5 Conclusion

425 This study reports the collection of experimental data for the SAMPL6 Part II log *P* Blind Prediction Challenge. In the physico-
426 chemical property prediction challenge components of SAMPL6, we aimed to separately evaluate performance of computational
427 methods for predicting ionization (pK_a) and nonaqueous partitioning (log *P*) of small molecules, collecting experimental data for
428 these properties on the same set of compounds and fielding sequential, independent prediction challenges. While we attempted
429 to measure octanol-water log *P* for all compounds in the SAMPL6 pK_a Challenge set—consisting of 24 compounds that resemble
430 fragments of kinase inhibitors—experimental limitations of the Sirius T3 potentiometric log *P* method meant that reliable log *P*
431 measurements could only be performed for 11 of these compounds. The resulting compound set had measured log *P* values in
432 the range of 1.95–4.09. This set included six molecules with 4-aminoquinazoline scaffolds, and two molecules with benzimidazole
433 scaffolds. Although the chemical diversity and number of compounds was rather limited, blind high-quality log *P* datasets are
434 rare, and still highly valuable for evaluating the performance of computational predictions. Therefore, the SAMPL6 Part II log *P*
435 Blind Prediction Challenge was held between November 1, 2018 and March 22, 2019 using the log *P* measurements presented in
436 this paper. This dataset can be utilized as part of a benchmark set for the assessment of future log *P* predictions methods.

437 6 Code and data availability

438 All SAMPL6 log *P* Challenge instructions, submissions, experimental data and analysis are available at
439 https://github.com/samplchallenges/SAMPL6/tree/master/physical_properties/logP

440 7 Overview of Supplementary Information

441 Supplementary tables and figures appearing in the Supplementary Information document

- 442 • **Table S1:** Procurement details of SAMPL6 Part II log *P* Challenge compounds.
- 443 • **Table S2:** Replicate potentiometric log *P* measurements performed with Sirius T3 for octanol and ISA water biphasic system.
- 444 • **Table S3:** SMILES and InChI identifiers of SAMPL6 log *P* Challenge molecules.

- 445 • **Table S4:** Molecules from the SAMPL6 pK_a Challenge not included in the SAMPL6 log P Challenge.
- 446 • **Figure S1:** HRMS determination of SM13 molecular weight.
- 447 • **Figure S2:** NMR determination of SM13 structure.

448 Additional supplementary files

449 *logP_experiment_reports.zip* file includes:

- 450 • Sirius T3 reports for all measurements in PDF and T3 formats: log P measurements of SAMPL6 log P Challenge set and
- 451 cosolvent pK_a measurements of SM14, SM15, and SM16.
- 452 • Table 1 in CSV format (*logP_experimental_values.csv*)
- 453 • Table S2 in CSV format (*replicate-logP-measurements-table.csv*)
- 454 • Table S3 in CSV format (*chemical-identifiers-table.csv*)
- 455 • Table S4 in CSV format (*molecules_with_unsuccessful_logP_measurements.csv*)

456 8 Author Contributions

457 Conceptualization, MI, JDC, TR, DLM ; Methodology, MI, DL ; Software, MI ; Formal Analysis, MI ; Investigation, MI, DL; Resources,

458 TR, DL; Data Curation, MI ; Writing-Original Draft, MI, DL; Writing - Review and Editing, MI, DL, JDC, TR, DLM; Visualization, MI ;

459 Supervision, JDC, TR, DLM ; Project Administration, MI ; Funding Acquisition, DLM, JDC, TR, MI.

461 9 Acknowledgments

462 MI and JDC acknowledge support from the Sloan Kettering Institute. JDC acknowledges partial support from NIH grant P30

463 CA008748. MI, JDC, ASR, and DLM gratefully acknowledge support from NIH grant R01GM124270 supporting the SAMPL Blind

464 Challenges. MI acknowledges support from a Doris J. Hutchinson Fellowship. DLM appreciates financial support from the National

465 Institutes of Health (1R01GM108889-01), the National Science Foundation (CHE 1352608). The authors are extremely grateful

466 for the assistance and support from the MRL Preformulations and NMR Structure Elucidation groups for materials, expertise,

467 and instrument time, without which this SAMPL challenge would not have been possible. The authors would like to thank

468 Ryan Cohen from the NMR Structure Elucidation group for the NMR and LC-MS analysis of SM13. MI and DL are grateful to

469 Pion/Sirius Analytical for their technical support in the planning and execution of this study. We are especially thankful to Karl Box

470 (Sirius Analytical) for the guidance on optimization and interpretation of log P measurements with the Sirius T3. We thank Brad

471 Sherborne (MRL; ORCID: [0000-0002-0037-3427](https://orcid.org/0000-0002-0037-3427)) for his valuable insights at the conception of the log P challenge and connecting

472 us with TR and DL who were able to provide resources for experimental measurements. We acknowledge contributions from

473 Caitlin Bannan who provided feedback on experimental data collection and structure of log P challenge from a computational

474 chemist's perspective. MI and JDC are grateful to OpenEye Scientific for providing a free academic software license for use in this

475 work. The content is solely the responsibility of the authors and does not necessarily represent the official views of the National

476 Institutes of Health. We thank anonymous reviewers for their input and constructive comments that improved this manuscript.

477 Research reported in this publication was supported by National Institute for General Medical Sciences of the National

478 Institutes of Health under award number R01GM124270 and R01GM108889, and from the National Cancer Institute of the

479 National Institutes of Health under P30CA008748.

480 10 Disclaimers

481 The content is solely the responsibility of the authors and does not necessarily represent the official views of the National

482 Institutes of Health.

483 11 Disclosures

484 JDC was a member of the Scientific Advisory Board for Schrödinger, LLC during part of this study. JDC and DLM are current

485 members of the Scientific Advisory Board of OpenEye Scientific Software. The Chodera laboratory receives or has received funding

486 from multiple sources, including the National Institutes of Health, the National Science Foundation, the Parker Institute for Cancer

487 Immunotherapy, Relay Therapeutics, Entasis Therapeutics, Silicon Therapeutics, EMD Serono (Merck KGaA), AstraZeneca, Vir

488 Biosciences, XtalPi, the Molecular Sciences Software Institute, the Starr Cancer Consortium, the Open Force Field Consortium,

489 Cycle for Survival, a Louis V. Gerstner Young Investigator Award, The Einstein Foundation, and the Sloan Kettering Institute. A
490 complete list of funding can be found at <http://choderalab.org/funding>.

491 References

- 492 [1] **Mobley DL**, Chodera JD, Isaacs L, Gibb BC. Advancing predictive modeling through focused development of model systems to drive new
493 modeling innovations. UC Irvine: Department of Pharmaceutical Sciences, UCI. 2016; <https://escholarship.org/uc/item/7cf8c6cr>.
- 494 [2] **Nicholls A**, Mobley DL, Guthrie JP, Chodera JD, Bayly CI, Cooper MD, Pande VS. Predicting Small-Molecule Solvation Free Energies: An
495 Informal Blind Test for Computational Chemistry. *J Med Chem*. 2008 Feb; 51(4):769–779. doi: [10.1021/jm070549+](https://doi.org/10.1021/jm070549+).
- 496 [3] **Guthrie JP**. A Blind Challenge for Computational Solvation Free Energies: Introduction and Overview. *J Phys Chem B*. 2009 Jan; 113(14):4501–
497 4507. doi: [10.1021/jp806724u](https://doi.org/10.1021/jp806724u).
- 498 [4] **Skillman AG**, Geballe MT, Nicholls A. SAMPL2 Challenge: Prediction of Solvation Energies and Tautomer Ratios. *J Comput Aided Mol Des*.
499 2010 Apr; 24(4):257–258. doi: [10.1007/s10822-010-9358-0](https://doi.org/10.1007/s10822-010-9358-0).
- 500 [5] **Geballe MT**, Skillman AG, Nicholls A, Guthrie JP, Taylor PJ. The SAMPL2 Blind Prediction Challenge: Introduction and Overview. *J Comput*
501 *Aided Mol Des*. 2010 May; 24(4):259–279. doi: [10.1007/s10822-010-9350-8](https://doi.org/10.1007/s10822-010-9350-8).
- 502 [6] **Skillman AG**. SAMPL3: Blinded Prediction of Host–guest Binding Affinities, Hydration Free Energies, and Trypsin Inhibitors. *J Comput Aided*
503 *Mol Des*. 2012 May; 26(5):473–474. doi: [10.1007/s10822-012-9580-z](https://doi.org/10.1007/s10822-012-9580-z).
- 504 [7] **Geballe MT**, Guthrie JP. The SAMPL3 Blind Prediction Challenge: Transfer Energy Overview. *J Comput Aided Mol Des*. 2012 Apr; 26(5):489–496.
505 doi: [10.1007/s10822-012-9568-8](https://doi.org/10.1007/s10822-012-9568-8).
- 506 [8] **Muddana HS**, Varnado CD, Bielawski CW, Urbach AR, Isaacs L, Geballe MT, Gilson MK. Blind Prediction of Host–guest Binding Affinities: A
507 New SAMPL3 Challenge. *J Comput Aided Mol Des*. 2012 Feb; 26(5):475–487. doi: [10.1007/s10822-012-9554-1](https://doi.org/10.1007/s10822-012-9554-1).
- 508 [9] **Guthrie JP**. SAMPL4, a Blind Challenge for Computational Solvation Free Energies: The Compounds Considered. *J Comput Aided Mol Des*.
509 2014 Apr; 28(3):151–168. doi: [10.1007/s10822-014-9738-y](https://doi.org/10.1007/s10822-014-9738-y).
- 510 [10] **Mobley DL**, Wymer KL, Lim NM, Guthrie JP. Blind Prediction of Solvation Free Energies from the SAMPL4 Challenge. *J Comput Aided Mol Des*.
511 2014 Mar; 28(3):135–150. doi: [10.1007/s10822-014-9718-2](https://doi.org/10.1007/s10822-014-9718-2).
- 512 [11] **Muddana HS**, Fenley AT, Mobley DL, Gilson MK. The SAMPL4 Host–guest Blind Prediction Challenge: An Overview. *J Comput Aided Mol Des*.
513 2014 Mar; 28(4):305–317. doi: [10.1007/s10822-014-9735-1](https://doi.org/10.1007/s10822-014-9735-1).
- 514 [12] **Mobley DL**, Liu S, Lim NM, Wymer KL, Perryman AL, Forli S, Deng N, Su J, Branson K, Olson AJ. Blind Prediction of HIV Integrase Binding from
515 the SAMPL4 Challenge. *J Comput Aided Mol Des*. 2014 Mar; 28(4):327–345. doi: [10.1007/s10822-014-9723-5](https://doi.org/10.1007/s10822-014-9723-5).
- 516 [13] **Yin J**, Henriksen NM, Slochower DR, Shirts MR, Chiu MW, Mobley DL, Gilson MK. Overview of the SAMPL5 Host–guest Challenge: Are We
517 Doing Better? *J Comput Aided Mol Des*. 2017; 31(1):1–19. doi: [10.1007/s10822-016-9974-4](https://doi.org/10.1007/s10822-016-9974-4).
- 518 [14] **Bannan CC**, Burley KH, Chiu M, Shirts MR, Gilson MK, Mobley DL. Blind Prediction of Cyclohexane–water Distribution Coefficients from the
519 SAMPL5 Challenge. *J Comput Aided Mol Des*. 2016 Sep; 30(11):1–18. doi: [10.1007/s10822-016-9954-8](https://doi.org/10.1007/s10822-016-9954-8).
- 520 [15] **Rizzi A**, Murkli S, McNeill JN, Yao W, Sullivan M, Gilson MK, Chiu MW, Isaacs L, Gibb BC, Mobley DL, et al. Overview of the SAMPL6 host–guest
521 binding affinity prediction challenge. *Journal of computer-aided molecular design*. 2018; 32(10):937–963.
- 522 [16] **Muddana HS**, Gilson MK. Prediction of SAMPL3 Host–guest Binding Affinities: Evaluating the Accuracy of Generalized Force-Fields. *J Comput*
523 *Aided Mol Des*. 2012 Jan; 26(5):517–525. doi: [10.1007/s10822-012-9544-3](https://doi.org/10.1007/s10822-012-9544-3).
- 524 [17] **Gibb CLD**, Gibb BC. Binding of Cyclic Carboxylates to Octa-Acid Deep-Cavity Cavitand. *J Comput Aided Mol Des*. 2013 Nov; 28(4):319–325.
525 doi: [10.1007/s10822-013-9690-2](https://doi.org/10.1007/s10822-013-9690-2).
- 526 [18] **Cao L**, Isaacs L. Absolute and Relative Binding Affinity of Cucurbit[7]Urils towards a Series of Cationic Guests. *Supramol Chem*. 2014 Mar;
527 26(3-4):251–258. doi: [10.1080/10610278.2013.852674](https://doi.org/10.1080/10610278.2013.852674).
- 528 [19] **Sullivan MR**, Sokkalingam P, Nguyen T, Donahue JP, Gibb BC. Binding of Carboxylate and Trimethylammonium Salts to Octa-Acid and TEMOA
529 Deep-Cavity Cavitands. *J Comput Aided Mol Des*. 2017; 31(1):1–8. doi: [10.1007/s10822-016-9925-0](https://doi.org/10.1007/s10822-016-9925-0).
- 530 [20] **Bannan CC**, Burley KH, Chiu M, Shirts MR, Gilson MK, Mobley DL. Blind prediction of cyclohexane–water distribution coefficients from
531 the SAMPL5 challenge. *Journal of Computer-Aided Molecular Design*. 2016 Nov; 30(11):927–944. [http://link.springer.com/10.1007/](http://link.springer.com/10.1007/s10822-016-9954-8)
532 [s10822-016-9954-8](https://doi.org/10.1007/s10822-016-9954-8), doi: [10.1007/s10822-016-9954-8](https://doi.org/10.1007/s10822-016-9954-8).

- 533 [21] **Rustenburg AS**, Dancer J, Lin B, Feng JA, Ortwine DF, Mobley DL, Chodera JD. Measuring experimental cyclohexane-water distribution
534 coefficients for the SAMPL5 challenge. *Journal of Computer-Aided Molecular Design*. 2016 Nov; 30(11):945–958. <http://link.springer.com/10.1007/s10822-016-9971-7>, doi: 10.1007/s10822-016-9971-7.
- 536 [22] **Waring MJ**. Lipophilicity in drug discovery. *Expert Opinion on Drug Discovery*. 2010 Mar; 5(3):235–248. <http://www.tandfonline.com/doi/full/10.1517/17460441003605098>, doi: 10.1517/17460441003605098.
- 538 [23] **Lipinski CA**, Lombardo F, Dominy BW, Feeney PJ. Experimental and computational approaches to estimate solubility and permeability in
539 drug discovery and development settings. *Advanced Drug Delivery Reviews*. 1997; 23(1):3 – 25. <http://www.sciencedirect.com/science/article/pii/S0169409X96004231>, doi: [https://doi.org/10.1016/S0169-409X\(96\)00423-1](https://doi.org/10.1016/S0169-409X(96)00423-1).
- 541 [24] **Leo A**, Hansch C, Elkins D. Partition coefficients and their uses. *Chemical Reviews*. 1971 Dec; 71(6):525–616. <http://pubs.acs.org/doi/abs/10.1021/cr60274a001>, doi: 10.1021/cr60274a001.
- 543 [25] **Arnott JA**, Planey SL. The influence of lipophilicity in drug discovery and design. *Expert Opinion on Drug Discovery*. 2012 Oct; 7(10):863–875.
544 <http://www.tandfonline.com/doi/full/10.1517/17460441.2012.714363>, doi: 10.1517/17460441.2012.714363.
- 545 [26] **Lipnick RL**. Environmental Hazard Assessment Using Lipophilicity Data. In: Pliška V, Testa B, van de Waterbeemd H, editors. *Methods
546 and Principles in Medicinal Chemistry* Weinheim, Germany: Wiley-VCH Verlag GmbH; 2008.p. 339–353. <http://doi.wiley.com/10.1002/9783527614998.ch19>, doi: 10.1002/9783527614998.ch19.
- 548 [27] **Pickard FC**, König G, Tofoleanu F, Lee J, Simmonett AC, Shao Y, Ponder JW, Brooks BR. Blind Prediction of Distribution in the SAMPL5
549 Challenge with QM Based Protomer and pKa Corrections. *J Comput Aided Mol Des*. 2016 Sep; 30(11):1–14. doi: 10.1007/s10822-016-9955-7.
- 550 [28] **Işık M**, Bergazin TD, Fox T, Rizzi A, Chodera JD, Mobley DL. Assessing the Accuracy of Octanol-Water Partition Coefficient Predictions in the
551 SAMPL6 Part II logP Challenge. *Journal of Computer-Aided Molecular Design*. 2019; (SAMPL6 Part II Special Issue).
- 552 [29] **Işık M**, Levorse D, Rustenburg AS, Ndukwe IE, Wang H, Wang X, Reibarkh M, Martin GE, Makarov AA, Mobley DL, Rhodes T, Chodera JD.
553 pKa measurements for the SAMPL6 prediction challenge for a set of kinase inhibitor-like fragments. *Journal of Computer-Aided Molecular
554 Design*. 2018 Oct; 32(10):1117–1138. <http://link.springer.com/10.1007/s10822-018-0168-0>, doi: 10.1007/s10822-018-0168-0.
- 555 [30] **Tsuji A**, Kubo O, Miyamoto E, Yamana T. Physicochemical Properties of β -Lactam Antibiotics: Oil-Water Distribution. *Journal of Pharmaceutical
556 Sciences*. 1977 Dec; 66(12):1675–1679. doi: 10.1002/jps.2600661205.
- 557 [31] **Avdeef A**, Box KJ, Comer JEA, Hibbert C, Tam KY. pH-Metric logP 10. Determination of Liposomal Membrane-Water Partition Coefficients of
558 Lonizable Drugs. *Pharmaceutical Research*. 1998 Feb; 15(2):209–215. doi: 10.1023/A:1011954332221.
- 559 [32] Octanol-Water Partitioning. In: *Absorption and Drug Development* Hoboken, NJ, USA: John Wiley & Sons, Inc.; 2012.p. 174–219. doi:
560 10.1002/9781118286067.ch4.
- 561 [33] OECD, Test No. 107: Partition Coefficient (n-octanol/water): Shake Flask Method, OECD Guidelines for the Testing of Chemicals, Section 1,
562 OECD Publishing, Paris; 1995. doi: <https://doi.org/10.1787/9789264069626-en>.
- 563 [34] **Hitzel L**, Watt AP, Locker KL. An Increased Throughput Method for the Determination of Partition Coefficients. *Pharmaceutical Research*.
564 2000 Nov; 17(11):1389–1395. <https://doi.org/10.1023/A:1007546905874>, doi: 10.1023/A:1007546905874.
- 565 [35] **Lin B**, Pease JH. A Novel Method for High Throughput Lipophilicity Determination by Microscale Shake Flask and Liquid Chromatography
566 Tandem Mass Spectrometry. *Combinatorial Chemistry High Throughput Screening*. 2013; 16(10):817–825. [http://www.eurekaselect.com/
567 node/114332/article](http://www.eurekaselect.com/node/114332/article), doi: 10.2174/1386207311301010007.
- 568 [36] **De Bruijn J**, Busser F, Seinen W, Hermens J. Determination of octanol/water partition coefficients for hydrophobic organic chemicals with
569 the “slow-stirring” method. *Environmental Toxicology and Chemistry*. 1989; 8(6):499–512. <https://setac.onlinelibrary.wiley.com/doi/abs/10.1002/etc.5620080607>, doi: 10.1002/etc.5620080607.
- 571 [37] **Andersson JT**, Schröder W. A Method for Measuring 1-Octanol/Water Partition Coefficients. *Analytical Chemistry*. 1999 Aug; 71(16):3610–3614.
572 <https://pubs.acs.org/doi/10.1021/ac9902291>, doi: 10.1021/ac9902291.
- 573 [38] **Herbert BJ**, Dorsey JG. n-Octanol-Water Partition Coefficient Estimation by Micellar Electrokinetic Capillary Chromatography. *Analytical
574 Chemistry*. 1995 Feb; 67(4):744–749. <http://pubs.acs.org/doi/abs/10.1021/ac00100a009>, doi: 10.1021/ac00100a009.
- 575 [39] **Berthod A**, Carda-Broch S. Determination of liquid-liquid partition coefficients by separation methods. *Journal of Chromatography A*. 2004
576 May; 1037(1-2):3–14. <https://linkinghub.elsevier.com/retrieve/pii/S0021967304000445>, doi: 10.1016/j.chroma.2004.01.001.
- 577 [40] **McCall JM**. Liquid-liquid partition coefficients by high-pressure liquid chromatography. *Journal of Medicinal Chemistry*. 1975 Jun; 18(6):549–
578 552. <http://pubs.acs.org/doi/abs/10.1021/jm00240a003>, doi: 10.1021/jm00240a003.

- 579 [41] **Unger SH**, Cook JR, Hollenberg JS. Simple Procedure for Determining Octanol–Aqueous Partition, Distribution, and Ionization Coefficients
580 by Reversed-Phase High-Pressure Liquid Chromatography. *Journal of Pharmaceutical Sciences*. 1978 Oct; 67(10):1364–1367. <https://linkinghub.elsevier.com/retrieve/pii/S0022354915422609>, doi: 10.1002/jps.2600671008.
- 582 [42] **Valkó K**, Bevan C, Reynolds D. Chromatographic Hydrophobicity Index by Fast-Gradient RP-HPLC: A High-Throughput Alternative to log P/log
583 D. *Analytical Chemistry*. 1997 Jun; 69(11):2022–2029. <https://pubs.acs.org/doi/10.1021/ac961242d>, doi: 10.1021/ac961242d.
- 584 [43] **Valkó K**. General Approach for the Estimation of Octanol/Water Partition Coefficient by Reversed-Phase High-Performance Liquid Chromatography. *Journal of Liquid Chromatography*. 1984; 7(7):1405–1424. doi: 10.1080/01483918408074054.
- 586 [44] OECD, Test No. 117: Partition Coefficient (n-octanol/water): HPLC Method, OECD Guidelines for the Testing of Chemicals, Section 1, OECD
587 Publishing, Paris; 2004. doi: <https://doi.org/10.1787/9789264069824-en>.
- 588 [45] **Takacs-Novak K**, Avdeef A. Interlaboratory study of log P determination by shake-flask and potentiometric methods. *Journal of Pharmaceutical and Biomedical Analysis*. 1996; 14:1405–1413.
- 590 [46] **Avdeef A**. PH-metric log P. Part 1. Difference plots for determining ion-pair octanol-water partition coefficients of multiprotic substances. *Quantitative Structure-Activity Relationships*. 1992; 11(4):510–517.
- 592 [47] Sirius T3 User Manual, v1.1; 2008. Sirius Analytical Instruments Ltd, East Sussex, UK.
- 593 [48] **Avdeef A**. pH-metric log P. II: Refinement of partition coefficients and ionization constants of multiprotic substances. *Journal of pharmaceutical sciences*. 1993; 82(2):183–190.
- 595 [49] **Slater B**, McCormack A, Avdeef A, Comer JE. Ph-metric log P. 4. Comparison of partition coefficients determined by HPLC and potentiometric
596 methods to literature values. *Journal of pharmaceutical sciences*. 1994; 83(9):1280–1283.
- 597 [50] **Comer J**, Tam K. Lipophilicity profiles: theory and measurement. Wiley-VCH: Zürich, Switzerland; 2001.
- 598 [51] OECD Guideline 122: Partition Coefficient (n-Octanol/Water), pH-Metric Method for Ionisable Substances,;. Revised Draft. Nov.2000.
- 599 [52] **Işik M**, Rustenburg A, Rizzi A, Bannan C, Gunner MR, Mobley DL, Chodera JD. Accuracy of macroscopic and microscopic pKa predictions of
600 small molecules evaluated by the SAMPL6 blind prediction challenge. *Journal of Computer-Aided Molecular Design*. 2019; Manuscript in
601 preparation.
- 602 [53] **Wishart DS**. DrugBank: a comprehensive resource for in silico drug discovery and exploration. *Nucleic Acids Research*. 2006 Jan;
603 34(90001):D668–D672. <https://academic.oup.com/nar/article-lookup/doi/10.1093/nar/gkj067>, doi: 10.1093/nar/gkj067.
- 604 [54] **Pence HE**, Williams A. ChemSpider: An Online Chemical Information Resource. *Journal of Chemical Education*. 2010 Nov; 87(11):1123–1124.
605 <http://pubs.acs.org/doi/abs/10.1021/ed100697w>, doi: 10.1021/ed100697w.
- 606 [55] NCI Open Database, August 2006 Release,;. <https://cactus.nci.nih.gov/download/nci/>.
- 607 [56] Enhanced NCI Database Browser 2.2,;. <https://cactus.nci.nih.gov/ncidb2.2/>.
- 608 [57] **Kim S**, Thiessen PA, Bolton EE, Chen J, Fu G, Gindulyte A, Han L, He J, He S, Shoemaker BA, Wang J, Yu B, Zhang J, Bryant SH. PubChem
609 Substance and Compound databases. *Nucleic Acids Research*. 2016 Jan; 44(D1):D1202–D1213. <https://academic.oup.com/nar/article-lookup/doi/10.1093/nar/gkv951>,
610 doi: 10.1093/nar/gkv951.
- 611 [58] **Tam KY**, Takács-Novák K. Multi-wavelength spectrophotometric determination of acid dissociation constants: a validation study. *Analytica Chimica Acta*. 2001 Apr; 434(1):157–167. <https://linkinghub.elsevier.com/retrieve/pii/S0003267001008108>, doi: 10.1016/S0003-
612 2670(01)00810-8.
- 614 [59] **Allen RI**, Box KJ, Comer JEA, Peake C, Tam KY. Multiwavelength spectrophotometric determination of acid dissociation constants of
615 ionizable drugs. *Journal of Pharmaceutical and Biomedical Analysis*. 1998 Aug; 17(4-5):699–712. <https://linkinghub.elsevier.com/retrieve/pii/S0731708598000107>,
616 doi: 10.1016/S0731-7085(98)00010-7.
- 617 [60] **Ahn S**, Fessler JA. Standard errors of mean, variance, and standard deviation estimators. EECs Department, The University of Michigan.
618 2003; p. 1–2. <http://web.eecs.umich.edu/~fessler/papers/lists/files/tr/stderr.pdf>.
- 619 [61] OEDepict Toolkit 2017.Feb.1;. OpenEye Scientific Software, Santa Fe, NM. <http://www.eyesopen.com>.
- 620 [62] **Takács-Novák K**, Avdeef A, Box KJ, Podányi B, Szász G. Determination of Protonation Macro- and Microconstants and Octanol/Water Partition
621 Coefficient of the Antiinflammatory Drug Niflumic Acid. *Journal of Pharmaceutical and Biomedical Analysis*. 1994 Nov; 12(11):1369–1377.
622 doi: 10.1016/0731-7085(94)00090-5.

- 623 [63] **Port A**, Bordas M, Enrech R, Pascual R, Rosés M, Ràfols C, Subirats X, Bosch E. Critical Comparison of Shake-Flask, Potentiometric and
624 Chromatographic Methods for Lipophilicity Evaluation (Log P_{o/w}) of Neutral, Acidic, Basic, Amphoter, and Zwitterionic Drugs. European
625 Journal of Pharmaceutical Sciences. 2018 Sep; 122:331–340. doi: [10.1016/j.ejps.2018.07.010](https://doi.org/10.1016/j.ejps.2018.07.010).
- 626 [64] **Tielker N**, Tomazic D, Eberlein L, Güssregen S, Kast SM. The SAMPL6 challenge on predicting octanol-water partition coefficients from
627 ECRISM theory. Journal of Computer-Aided Molecular Design. 2019; (SAMPL6 Part II Special Issue).

628 **12 Supplementary Information**

Table S1. Procurement details of SAMPL6 Part II Octanol-Water Partition Coefficient Challenge compounds. ¹ Purities for these compounds were determined by LC-MS methods and reported elsewhere [29].

SAMPL6 Part II Molecule ID	Supplier	Lot no	Cat no	Supplier Reported Purity	Purity Detected by LC-MS	CAS no	eMolecules ID
SM02	ChemDiv	CM02432403	3232-0333		97.62%		1327907
SM04	ChemDiv		Z126957826		99.88%		30719859
SM07	Enamine	2017-0168841	Z57161635	95%	99.38%	100818-54-0	1327878
SM08	Enamine	2017-0168838	Z57157353	95%	99.24%	65418_08_8	1367649
SM09	Enamine	2017_0168839	Z220564816	95%	98.97%		1865544
SM11	Maybridge	142989	RJC00689SC	90%	98.02%	5334-30-5	719540
SM12	Maybridge	265423	DP00818SC		98.13%		1859493
SM13	Maybridge	248841	GK03474SC		97.51%		5828805
SM14	Enamine		Z57290870		96.48%		31653344
SM15	Enamine		Z1318268952		98.70%		37095168
SM16	VitaScreen		STK098832		97.73%		1284691

Table S2. Replicate potentiometric log *P* measurements performed with Sirius T3 for octanol and ISA water biphasic system. Three or four independent replicate experiments were performed starting from powder samples. Measurements were performed at $25.0 \pm 0.5^\circ\text{C}$ and in the presence of approximately 150 mM KCl to adjust ionic strength. A partitioning and ionization equilibrium model was fit to potentiometric measurements to estimate log *P* values of the neutral species and also the charged species. Experiments were optimized to be able to determine log *P* of neutral species with good precision. log *P* estimates of charged species have high variance between replicates and is unreliable.

SAMPL6 Molecule ID	Experimental Molecule ID	log <i>P</i> , +1 charged	log <i>P</i> , neutral	log <i>P</i> , -1 charged	Experiment code	Target sample weight (mg)	Experiment ID	Experimental Report Filename in Supplementary Info
SM02	M02	1.32 +- 0.06	4.10 +- 0.03		EXP28-11	2 mg	18C-01011	SM02_18C-01011_M02_octanol_pH-metric high logP_report.pdf
SM02	M02	0.45 +- 0.04	4.08 +- 0.01		EXP29-11	2 mg	18C-03011	SM02_18C-03011_M02_octanol_pH-metric high logP_report.pdf
SM02	M02	0.59 +- 0.04	4.03 +- 0.01		EXP29-12	2 mg	18C-03012	SM02_18C-03012_M02_octanol_pH-metric high logP_report.pdf
SM02	M02	1.14 +- 0.04	4.16 +- 0.01		EXP30-15	2 mg	18C-06015	SM02_18C-06015_M02_octanol_pH-metric high logP_report.pdf
SM04	M04	0.82 +- 0.06	4.04 +- 0.02		EXP33-02	1.36 mg	18C-24002	SM04_18C-24002_M04_octanol_pH-metric high logP_report.pdf
SM04	M04	0.87 +- 0.03	3.95 +- 0.01		EXP33-03	1.36 mg	18C-24003	SM04_18C-24003_M04_octanol_pH-metric high logP_report.pdf
SM04	M04	0.77 +- 0.03	3.95 +- 0.02		EXP33-04	1.36 mg	18C-24004	SM04_18C-24004_M04_octanol_pH-metric high logP_report.pdf
SM07	M07	0.44 +- 0.03	3.29 +- 0.01		EXP28-11	1 mg	18B-28011	SM07_18B-28011_M07_octanol_pH-metric high logP_report.pdf
SM07	M07	-5.97 +- 0.89	3.14 +- 0.01		Exp28-012	1 mg	18B-28012	SM07_18B-28012_M07_octanol_pH-metric high logP_report.pdf
SM07	M07	0.31 +- 0.04	3.21 +- 0.01		Exp28-013	1 mg	18B-28013	SM07_18B-28013_M07_octanol_pH-metric high logP_report.pdf
SM08 ¹	M08		3.05 +- 0.01	-0.40 +- 0.05	EXP29-07	1 mg	18C-02007	SM08_18C-02007_M08_octanol_pH-metric high logP_report.pdf
SM08 ¹	M08		3.08 +- 0.01	-0.07 +- 0.05	EXP29-08	1 mg	18C-02008	SM08_18C-02008_M08_octanol_pH-metric high logP_report.pdf
SM08 ¹	M08		3.16 +- 0.01	0.23 +- 0.03	EXP29-09	1 mg	18C-02009	SM08_18C-02009_M08_octanol_pH-metric high logP_report.pdf
SM09	M09	-9.50 +- 0.85	2.90 +- 0.01		EXP29-10	1 mg	18C-02010	SM09_18C-02010_M09_octanol_pH-metric high logP_report.pdf
SM09	M09	1.05 +- 0.04	3.14 +- 0.01		EXP29-01	1 mg	18C-03001	SM09_18C-03001_M09_octanol_pH-metric high logP_report.pdf
SM09	M09	0.91 +- 0.07	3.05 +- 0.02		EXP30-07	1 mg	18C-06007	SM09_18C-06007_M09_octanol_pH-metric high logP_report.pdf
SM11	M11	-5.60 +- 1.55	2.09 +- 0.01		EXP27-16	1 mg	18B-27016	SM11_18B-27016_M11_octanol_pH-metric high logP_report.pdf
SM11	M11	0.55 +- 0.07	2.19 +- 0.02		Exp28-01	1.1 mg	18C-01001	SM11_18C-01001_M11_octanol_pH-metric high logP_report.pdf
SM11	M11	-3.66 +- 2.11	2.01 +- 0.02		Exp28-02	1.1 mg	18C-01002	SM11_18C-01002_M11_octanol_pH-metric high logP_report.pdf
SM11	M11	-0.33 +- 0.82	2.12 +- 0.01		EXP31-10	1.5 mg	18C-09010	SM11_18C-09010_M11_octanol_pH-metric high logP_report.pdf
SM12	M12	1.02 +- 0.07	3.79 +- 0.02		EXP28-12	1.5 mg	18C-01012	SM12_18C-01012_M12_octanol_pH-metric high logP_report.pdf
SM12	M12	-4.20 +- 1.91	3.81 +- 0.01		EXP29-13	2 mg	18C-03013	SM12_18C-03013_M12_octanol_pH-metric high logP_report.pdf
SM12	M12	0.62 +- 0.05	3.91 +- 0.01		EXP29-14	2 mg	18C-03014	SM12_18C-03014_M12_octanol_pH-metric high logP_report.pdf
SM12	M12	0.40 +- 0.06	3.80 +- 0.01		EXP29-15	2 mg	18C-03015	SM12_18C-03015_M12_octanol_pH-metric high logP_report.pdf
SM13 ²	M13	-4.95 +- 1.76	2.87 +- 0.01		EXP31-11	1.5 mg	18C-09011	SM13_18C-09011_M13_octanol_pH-metric high logP_report.pdf
SM13 ²	M13	-7.57 +- 1.49	2.89 +- 0.02		EXP32-16	1.5 mg	18C-16016	SM13_18C-16016_M13_octanol_pH-metric high logP_report.pdf
SM13 ³	M13	0.09 +- 0.08	2.99 +- 0.03		EXP34-10	1 mg	18C-26010	SM13_18C-26010_M13_octanol_pH-metric high logP_report.pdf
SM14	M15	-4.96 +- 2.15	1.92 +- 0.01		EXP27-02	2 mg	18B-28002	SM14_18B-28002_M15_octanol_pH-metric high logP_report.pdf
SM14	M15	-0.11 +- 0.20	1.92 +- 0.01		Exp28-04	2 mg	18C-01004	SM14_18C-01004_M15_octanol_pH-metric high logP_report.pdf
SM14	M15	-0.05 +- 0.07	1.93 +- 0.01		EXP28-05	2 mg	18C-01005	SM14_18C-01005_M15_octanol_pH-metric high logP_report.pdf
SM14	M15	0.28 +- 0.16	2.04 +- 0.02		EXP29-06	2 mg	18C-03006	SM14_18C-03006_M15_octanol_pH-metric high logP_report.pdf
SM15	M16	1.38 +- 1.07	3.14 +- 0.01		EXP28-07	1.5 mg	18C-01007	SM15_18C-01007_M16_octanol_pH-metric high logP_report.pdf
SM15	M16	-1.34	3.04		EXP28-08	1.5 mg	18C-01008	SM15_18C-01008_M16_octanol_pH-metric high logP_report.pdf
SM15	M16	-0.17 +- 0.20	3.04 +- 0.01		EXP28-09	1.5 mg	18C-01009	SM15_18C-01009_M16_octanol_pH-metric high logP_report.pdf
SM16 ²	M18	-0.24 +- 0.09	2.63 +- 0.01		EXP31-14	1.5 mg	18C-09014	SM16_18C-09014_M18_octanol_pH-metric high logP_report.pdf
SM16 ²	M18	-0.73 +- 0.56	2.59 +- 0.01		EXP31-15	1.5 mg	18C-09015	SM16_18C-09015_M18_octanol_pH-metric high logP_report.pdf
SM16 ²	M18	-0.21 +- 0.12	2.63 +- 0.02		EXP31-16	1.5 mg	18C-09016	SM16_18C-09016_M18_octanol_pH-metric high logP_report.pdf

¹ Sample predosed with 80 uL octanol to help with kinetic solubility issues.

² Sample predosed with 100 uL octanol to help with kinetic solubility issues.

³ Sample predosed with 200 uL octanol to help with kinetic solubility issues.

Table S3. SMILES and InChI identifiers of SAMPL6 log *P* Challenge molecules.

SAMPL6 Molecule ID	isomeric SMILES	InChI
SM02	<chem>c1ccc2c(c1)c(ncn2)Nc3cccc(c3)C(F)F</chem>	InChI=1S/C15H10F3N3/c16-15(17,18)10-4-3-5-11(8-10)21-14-12-6-1-2-7-13(12)19-9-20-14/h1-9H,(H,19,20,21)
SM04	<chem>c1ccc2c(c1)c(ncn2)Nc3ccc(cc3)Cl</chem>	InChI=1S/C15H12ClN3/c16-12-7-5-11(6-8-12)9-17-15-13-3-1-2-4-14(13)18-10-19-15/h1-8,10H,9H2,(H,17,18,19)
SM07	<chem>c1ccc(cc1)CNc2c3cccc3ncn2</chem>	InChI=1S/C15H13N3/c1-2-6-12(7-3-1)10-16-15-13-8-4-5-9-14(13)17-11-18-15/h1-9,11H,10H2,(H,16,17,18)
SM08	<chem>Cc1ccc2c(c1)c(c(=O)[nH]2)CC(=O)Oc3ccccc3</chem>	InChI=1S/C18H15NO3/c1-11-7-8-15-13(9-11)17(12-5-3-2-4-6-12)14(10-16(20)21)18(22)19-15/h2-9H,10H2,1H3,(H,19,22)(H,20,21)
SM09	<chem>COc1cccc(c1)Nc2c3cccc3ncn2.Cl</chem>	InChI=1S/C15H13N3O.ClH/c1-19-12-6-4-5-11(9-12)18-15-13-7-2-3-8-14(13)16-10-17-15;/h2-10H,1H3,(H,16,17,18);1H
SM11	<chem>c1ccc(cc1)n2c3c(nc2)c(ncn3)N</chem>	InChI=1S/C11H9N5/c12-10-9-6-15-16(11(9)14-7-13-10)8-4-2-1-3-5-8/h1-7H,(H2,12,13,14)
SM12	<chem>c1ccc2c(c1)c(ncn2)Nc3cccc(c3)Cl.Cl</chem>	InChI=1S/C14H10ClN3.ClH/c15-10-4-3-5-11(8-10)18-14-12-6-1-2-7-13(12)16-9-17-14;/h1-9H,(H,16,17,18);1H
SM13	<chem>Cc1cccc(c1)Nc2c3cc(c(cc3ncn2)OC)OC</chem>	InChI=1S/C17H17N3O2/c1-11-5-4-6-12(7-11)20-17-13-8-15(21-2)16(22-3)9-14(13)18-10-19-17/h4-10H,1-3H3,(H,18,19,20)
SM14	<chem>c1ccc(cc1)n2cnc3c2ccc(c3)N</chem>	InChI=1S/C13H11N3/c14-10-6-7-13-12(8-10)15-9-16(13)11-4-2-1-3-5-11/h1-9H,14H2
SM15	<chem>c1ccc2c(c1)ncn2c3ccc(cc3)O</chem>	InChI=1S/C13H10N2O/c16-11-7-5-10(6-8-11)15-9-14-12-3-1-2-4-13(12)15/h1-9,16H
SM16	<chem>c1cc(c(c1)Cl)C(=O)Nc2ccncc2)Cl</chem>	InChI=1S/C12H8Cl2N2O/c13-9-2-1-3-10(14)11(9)12(17)16-8-4-6-15-7-5-8/h1-7H,(H,15,16,17)

Table S4. Molecules from SAMPL6 pK_a Challenge not included in SAMPL6 log *P* Challenge. These are molecules for which potentiometric log *P* experiments could not be optimized. Suspected reasons why good log *P* measurements could not be collected for these molecules are listed in the "Limitation for potentiometric log *P*" column. Limitation of pK_a value indicates that apparent pK_a shifts outside of measurable range in the presence of the octanol phase. Solubility limitation indicates that we could not find a potentiometric log *P* protocol that can avoid precipitation issues. Experimental pK_a values were originally reported elsewhere [29].

SAMPL6 Molecule ID	Limitation for potentiometric log <i>P</i>	Experimental pK_a	SMILES	Experimental Molecule ID
SM01	pK_a	9.53 (acid)	<chem>c1cc2c(cc1O)c3c(o2)C(=O)NCCC3</chem>	M01
SM03	solubility	7.02 (acid)	<chem>c1ccc(cc1)C2nnc(s2)NC(=O)c3cccs3</chem>	M03
SM05	solubility	4.59 (base)	<chem>c1ccc(c(c1)NC(=O)c2ccc(o2)Cl)N3CCCC3</chem>	M05
SM06	solubility	3.03 (base), 11.74 (base)	<chem>c1cc2cccnc2c(c1)NC(=O)c3cc(cnc3)Br</chem>	M06
SM10	solubility	9.02 (base)	<chem>c1ccc(cc1)C(=O)NCC(=O)Nc2nc3cccc3s2</chem>	M10
SM17	pK_a and solubility	3.16 (base)	<chem>c1ccc(cc1)CSc2nnc(o2)c3ccncc3</chem>	M19
SM18	pK_a and solubility	2.15 (base), 9.58 (acid), 11.02 (acid)	<chem>c1ccc2c(c1)c(=O)[nH]c(n2)CCC(=O)Nc3ncc(s3)Cc4ccc(c(c4)F)F</chem>	D01
SM19	pK_a and solubility	9.56 (acid)	<chem>CCOC1ccc2c(c1)sc(n2)NC(=O)C3ccc(c(c3)Cl)Cl</chem>	D02
SM20	solubility	5.70 (base)	<chem>c1cc(cc(c1)OCc2ccc(cc2Cl)Cl)/C=C/3\N(=O)NC(=O)S3</chem>	D05
SM21	solubility	4.10 (base)	<chem>c1cc(c(c1)Br)Nc2c(cnc(n2)Nc3cccc(c3)Br)F</chem>	D06
SM22	solubility	2.40 (base), 7.43 (acid)	<chem>c1cc2c(cc(c(c2nc1)O))I</chem>	D07
SM23	solubility	5.45 (base)	<chem>CCOC(=O)c1ccc(cc1)Nc2cc(nc(n2)Nc3ccc(cc3)C(=O)OCC)C</chem>	D08
SM24	pK_a	2.60 (base)	<chem>COc1ccc(cc1)c2c3c(ncnc3oc2c4ccc(cc4)OC)NCCO</chem>	D09

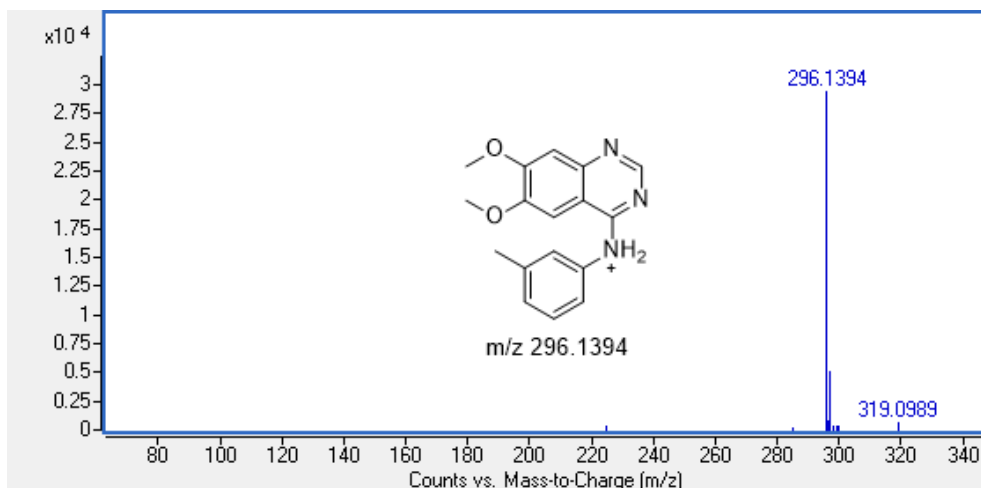


Figure S1. HRMS determination of SM13 molecular weight confirmed the supplier reported molecular weight.

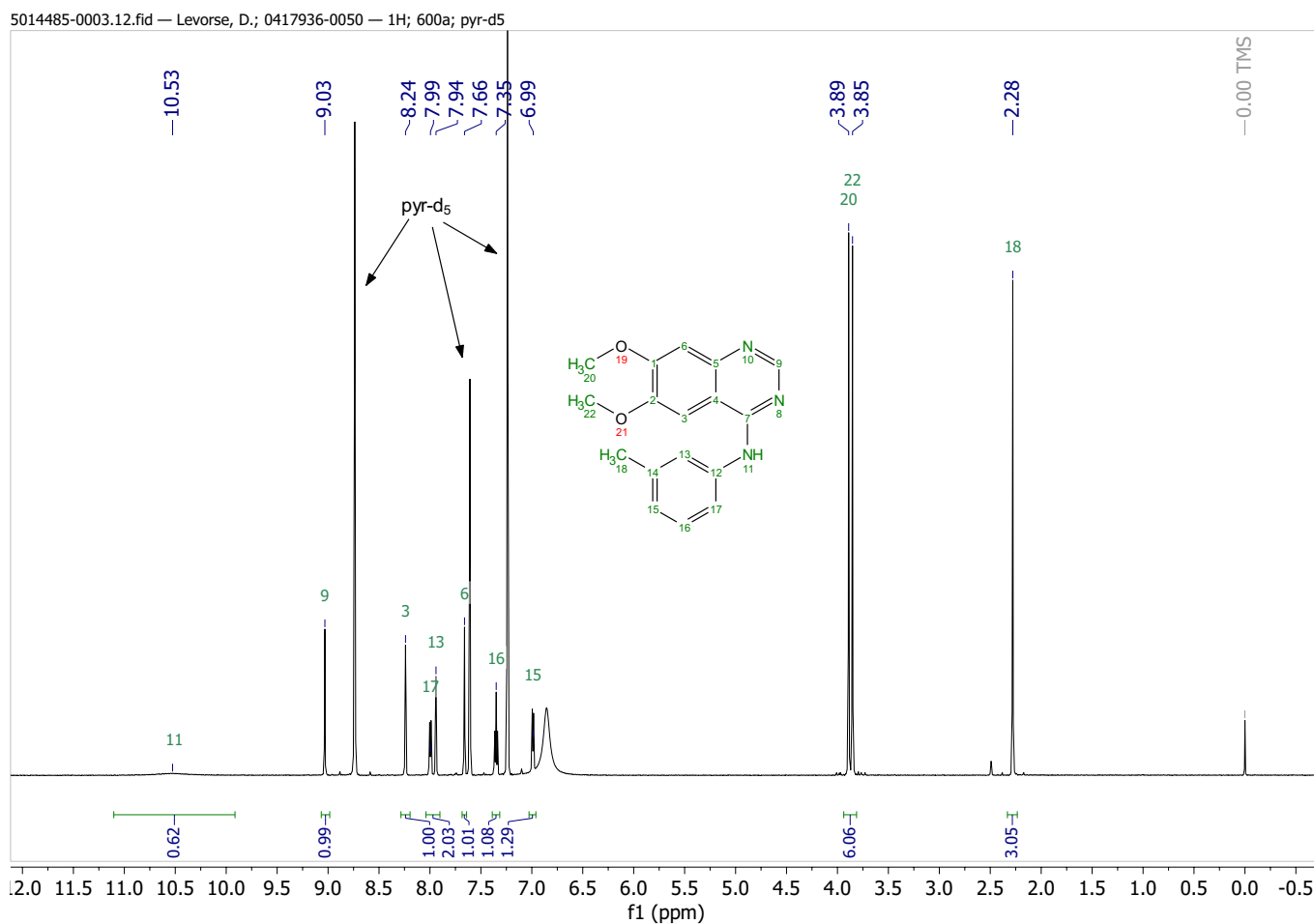


Figure S2. The ¹H 1D NMR spectrum of SM13 confirms compound identity and structure.